NPS ARCHIVE
1963
MAULDIN, J.

GRADUATE AERONAUTICAL LABORATORIES
CALIFORNIA INSTITUTE OF TECHNOLOGY

Firestone Flight Sciences Laboratory

Guggenheim Aeronautical Laboratory

Ka an Laboratory of Fluid Mechanics and Jet Propulsion

Thesis
M384

Pasadena

PART I. ANALYSIS OF A MULTI-STAGE AXIAL COMPRESSOR WITH HIGH REACTION BLADING

PART II. A DESIGN STUDY OF A MULTI-STAGE AXIAL COMPRESSOR WITH BLADING OF HIGH ASPECT RATIO

Thesis by

James H. Mauldin

Lieutenant, United States Navy

In Partial Fulfillment of the Requirements
For the Degree of
Aeronautical Engineer

California Institute of Technology
Pasadena, California
1963

DUDLEY KNOX LIBRARY
NAVAL POSTGRADUATE SCHOOL
MONTEREY CA 93943-5101

ARCHIVE
3
LDIN, J.

~~M384~~
~~2~~

ACKNOWLEDGMENTS

The author wishes to express his sincere appreciation to Dr. W. D. Rannie, who originally suggested the investigations in this thesis. His many hours of encouragement, guidance, and helpful criticism were invaluable during the course of this work.

Thanks are also due to Mrs. Roberta Duffy for typing the manuscript.

PART I. ANALYSIS OF A MULTI-STAGE AXIAL COMPRESSOR WITH HIGH REACTION BLADING

ABSTRACT FOR PART I

An analysis of a multi-stage axial compressor with high reaction blading is carried out. The usual methods of linearizing the equations for flow through the compressor fail for this type of blading. A numerical solution of the non-linear equations is worked through for off-design operation. Flow velocities through the first six stages are calculated for the off-design flow rates in order to insure that the flow does indeed come to a steady-state repeating pattern. Entering flow angles for both rotor and stator are calculated for this repeating flow condition. The off-design incidence angles for the stators at low flow rates indicate a possible deterioration of efficiency.

SUMMARY FOR PART I

The pressure rise per stage in an axial flow compressor is proportional to the square of the incidence velocity relative to the blades. Almost all axial compressors for gas turbines were designed with the whirl in the same direction as the rotor blade speed. This choice of design flow gave high efficiencies when the blades were designed properly. Until the introduction of transonic blading, a high efficiency was obtained only when the Mach number relative to the blade was less than unity -- usually in the neighborhood of 0.75. Relative velocities of this magnitude did not require whirl opposite to the direction of rotor blade speed and, in fact, the matching with a turbine was easier with whirl in the same direction as the rotor speed.

An axial compressor for a gas of low molecular weight, for instance helium, can be designed with blading similar to the axial compressor for air. However, the pressure rise per stage is proportional to the square of the Mach number of the relative velocity. The rotor blade rotational speed cannot be increased because of strength limitations, and hence the square of the relative Mach number and therefore the pressure ratio are decreased by a factor approximately proportional to the ratio of molecular weights. Thus, the number of stages required for a compressor using helium would be approximately seven times that for air for the same overall pressure. Clearly, higher relative velocities are required to decrease the number of stages for a gas of lower molecular weight. An obvious method of doing this is to introduce the whirl in the opposite direction to rotor blade speed.

A vortex flow pattern was chosen as the design condition: then the flow is truly two-dimensional; that is, there is no radial shift of the streamlines as the fluid proceeds downstream through the compressor.

This considerably simplifies the analysis of the flow at the design flow rate. Off-design calculations must still be carried out in order to investigate the compressor performance and to indicate how rapidly losses might increase as the compressor flow rate increases or decreases from the design value. For conventional multi-stage compressors with relatively low ideal pressure coefficients, this analysis is usually carried out by linearizing the governing equations for three-dimensional flow through the compressor, and is quite satisfactory. However, with whirl against the rotor blades and its correspondingly higher pressure coefficient, this type of linearization fails completely. It is necessary to allow for the streamline shift to avoid singularities in the solution. Thus, the full set of non-linear equatinns, taking into account the radial shift of the streamlines, must be used. In order to calculate the repeating flow pattern characteristic of multi-stage compressors, it was necessary to numerically determine the flow pattern through the first four or six stages.

Although detailed calculations of efficiency are scarcely possible, the results of the analysis can be used to give indications of probable losses. The degree of turning required by the blades appears to be within permissible limits. The off-design incidence angles for the rotors deviate very little from the design values. The stator incidence angles are more severe, and might produce a loss in efficiency over part of the stator blades.

I. INTRODUCTION

Conventional subsonic axial-flow compressors designed to use air as a working fluid are not necessarily suitable for gases of lower molecular weight. For a particular closed cycle system, where a working fluid other than air might be desirable, the number of stages required will vary greatly with the choice of gas. The number of stages is directly proportional to the specific heat at constant pressure and is inversely proportional to the blade speed and the change in tangential velocity of the gas through a stage. The blade speed is fixed by the strength of the blade material and is generally held as high as possible. With present-day air compressors, there is a maximum amount of tangential velocity change that can be accomplished efficiently. Thus, for a typical compressor designed to use air, the number of stages required would be increased approximately five times if a gas such as helium were used and the same temperature ratio across the compressor were to be maintained. This report describes a blade design that will hopefully reduce this high number of stages required for helium to approximately one-half the number presently used.

II. THEORY

Unlike conventional multi-stage compressors, the design of the stator blade is such as to give an accelerating flow through the stator rows. The rotor blades then turn the flow back to the axial direction. This type of design has been used in some single-stage fans. The notation to be used in this report is illustrated in Figure 1.

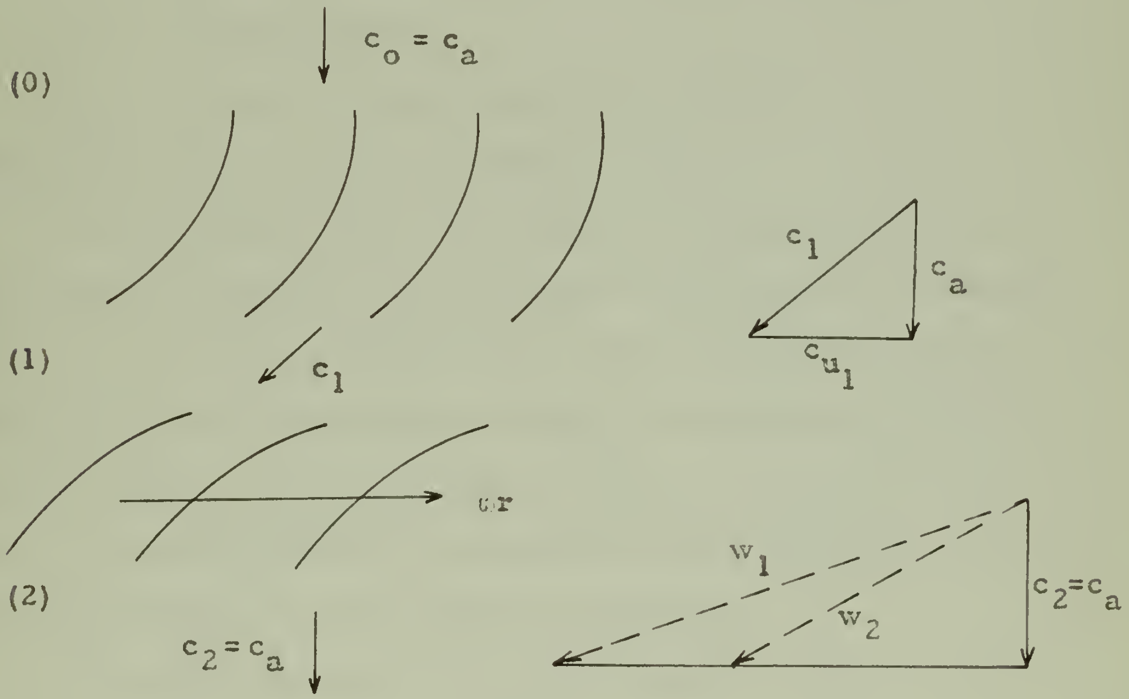

Figure 1.

The following list of symbols will be used throughout this report:

c_a = axial component of velocity

c_u = tangential component of velocity

c = absolute velocity

w = velocity relative to the rotor

w_u = tangential velocity relative to the rotor

γ = angle between axial direction and absolute velocities

β = angle between axial direction and relative velocities

R = tip radius

u = tip speed

ω = angular velocity of rotor

r = radius measured from compressor centerline

p = static pressure

ρ = density (assumed constant throughout)

Subscripts refer to stations as shown in Figure 1.

In "two-dimensional" flow through an axial compressor, the streamlines are assumed to lie on cylindrical surfaces with constant radii. The pressure gradients in the radial direction are ignored, although it is shown later that at design for vortex blading, the flow is two-dimensional and the pressure gradients are properly accounted for. Since an important difficulty in applying two-dimensional flow theory to this design arises, we will discuss it briefly here.

The blades are of the free vortex design. Thus

$$c_{u_1} \propto 1/r \ .$$

A dimensionless radius is defined by

$$\xi = r/R \ .$$

Therefore, the tangential component of velocity through the stator is taken as

$$c_{u_1} = u\alpha/\xi \ , \qquad (1)$$

where α is an arbitrary constant to be determined.

The pressure drop across a stator row is given by

$$\frac{p_1 - p_o}{\rho} = \tfrac{1}{2}(c_a^2 - c_1^2) \ . \qquad (2)$$

Since r is a constant along a streamline, the Bernoulli equation for rotating axes gives, for the pressure rise across a rotor row,

$$\frac{p_2 - p_1}{\rho} = \tfrac{1}{2}(w_1^2 - w_2^2) \ . \qquad (3)$$

The pressurerise across a stage is then

$$\frac{p_2 - p_o}{\rho} = \tfrac{1}{2}(w_1^2 - w_2^2 + c_a^2 - c_1^2) \, . \qquad (4)$$

At design, $c_{u_2} = 0$, and from the velocity diagrams we obtain

$$\begin{aligned}
w_{u_1} &= u\frac{\alpha}{\xi} + u\xi \\
w_{u_2} &= u\xi \\
w_1^2 &= c_a^2 + w_{u_1}^2 = c_a^2 + u^2\left(\frac{\alpha}{\xi} + \xi\right)^2 \\
w_2^2 &= c_a^2 + w_{u_2}^2 = c_a^2 + u^2\xi^2 \\
c_1^2 &= c_a^2 + c_{u_1}^2 = c_a^2 + u^2\left(\frac{\alpha}{\xi}\right)^2 \ .
\end{aligned}$$

After substitution of these relations into (4), we obtain, for the pressure rise across the stage,

$$\frac{p_2 - p_o}{\rho} = u^2\alpha \ . \qquad (5)$$

A work coefficient is usually defined as

$$\psi = \frac{\Delta p}{\frac{1}{2}\rho\,\omega^2 R^2} \ . \qquad (6)$$

Thus, when the compressor is operating at the design point,

$$\psi = 2\alpha \ .$$

However, α is not unrestricted. It has been found experimentally desirable (Ref. 1) to have

$$\frac{w_1^2 - w_2^2}{w_1^2} < \beta , \qquad (7)$$

where β is between 0.5 and 0.6. Defining a non-dimensional flow coefficient as

$$\phi = c_a/u , \qquad (8)$$

this restriction can be written

$$\frac{(\psi + 2\xi^2)^2}{4\xi^4/1-\beta} - \frac{\phi^2}{\xi^2/\beta} < 1 . \qquad (9)$$

This condition must be satisfied over the entire length of the blade. Since the restriction is most severe at the hub, values of ψ and ϕ evaluated there will be conservative over the rest of the blade. An existing experimental set-up prescribed the hub ratio $\xi_i = 0.6$. There is another restriction on the velocities that is not easily described in analytical form. This is the amount of turning that can be accomplished efficiently in the blade rows. Due to lower blade speed at the hub and the adverse pressure gradient in the rotor, this condition also is most severe at the rotor hub. β was chosen as 0.6, and values of the turning angle were obtained for different values of ψ. The quantities $\psi = 0.70$ and $\phi = 0.58$ were subsequently chosen. The value of ψ can be raised substantially for a compressor with hub ratio in the range 0.7 to 0.75.

So far, no difficulty with the two-dimensional theory has arisen. This is not unexpected since, as mentioned before, vortex blading is exactly two dimensional at the design flow rate. However, we have yet to consider the off-design conditions where a radial component of velocity does exist. At design, the work coefficient was constant over the blade height. This is desirable in order to cut down losses due to mix-

ing at the end of the compressor, and actually is necessary on all stages after the first few because a piling up of pressure at some radius is impossible for a very large number of stages. Thus, this restriction will be applied at off-design flow rates also. Then

$$\psi = \frac{\Delta p}{\frac{1}{2}\rho\omega^2 R^2} = \frac{1}{\omega^2 R^2}(w_1^{\,2} - w_2^{\,2} + c_2^{\,2} - c_1^{\,2}) = \text{constant.} \qquad (10)$$

Remembering that $c_{u_2} \neq 0$ for off-design conditions, then

$$w_{u_1} = u\xi + c_{u_1} ,$$

$$w_{u_2} = u\xi + c_{u_2} ,$$

and the work coefficient becomes

$$\psi = 2\frac{\xi}{u}(c_{u_1} - c_{u_2})$$

or

$$\psi = 2\xi[\xi + \phi(\tan\gamma_1 - \tan\beta_2)] \quad . \qquad (11)$$

A first approximation can be made that $\tan\gamma_1$ and $\tan\beta_2$, corresponding to the leaving angles of flow, are independent of the inlet angles and hence are independent of flow rate. If this is done, the local value of ϕ at the root is

$$\phi(\xi = 0.6) = \frac{0.72 - \psi}{1.2(\tan\beta_2 - \tan\gamma_1)} \quad . \qquad (12)$$

Since under our approximation $(\tan\beta_2 - \tan\gamma_1)$ is constant and is greater than zero, we see that for $\psi > 0.72$ the flow coefficient at the root becomes negative and is meaningless. If $\tan\beta_2$ and $\tan\gamma_1$ are allowed to change with flow speed and this change calculated by cascade theory, the singularity in ϕ is not relieved appreciably. Since values of the ideal pressure coefficient greater than 0.72 would be required in starting,

for instance, the two-dimensional analysis of the flow is unsatisfactory. It must be mentioned that if ψ could be pushed as high as 0.72 in a standard compressor, there would be the same difficulty. Normally, axial-flow air compressors have an ideal pressure coefficient of between 0.4 and 0.5 . It will be shown that a three-dimensional flow analysis of the compressor does not contain this singularity in ϕ . This difficulty is mathematical rather than physical, and appears to be the result of an invalid linearization of the three-dimensional equations of motion. There seems to be no way of calculating the ideal flow patterns except by a numerical procedure with a radial shift of the streamlines taken into account.

The assumptions made in the three-dimensional flow analysis are:

(1) incompressible perfect fluid;

(2) axisymmetric flow;

(3) equations are written for conditions far upstream and far downstream of a blade row.

The notation used is the same as in the two-dimensional analysis except that the odd subscripts refer to stations far downstream of stator rows and the even subscripts refer to stations far downstream of rotor rows (see Figure 2).

The Bernoulli equation for flow through a stator row is

$$\frac{2p_{2n+1}}{\rho} + c_{u_{2n+1}}^{2} + c_{a_{2n+1}}^{2} = \frac{2p_{2n}}{\rho} + c_{u_{2n}}^{2} + c_{a_{2n}}^{2} . \qquad (13)$$

The Bernoulli equation for flow through a rotor row is

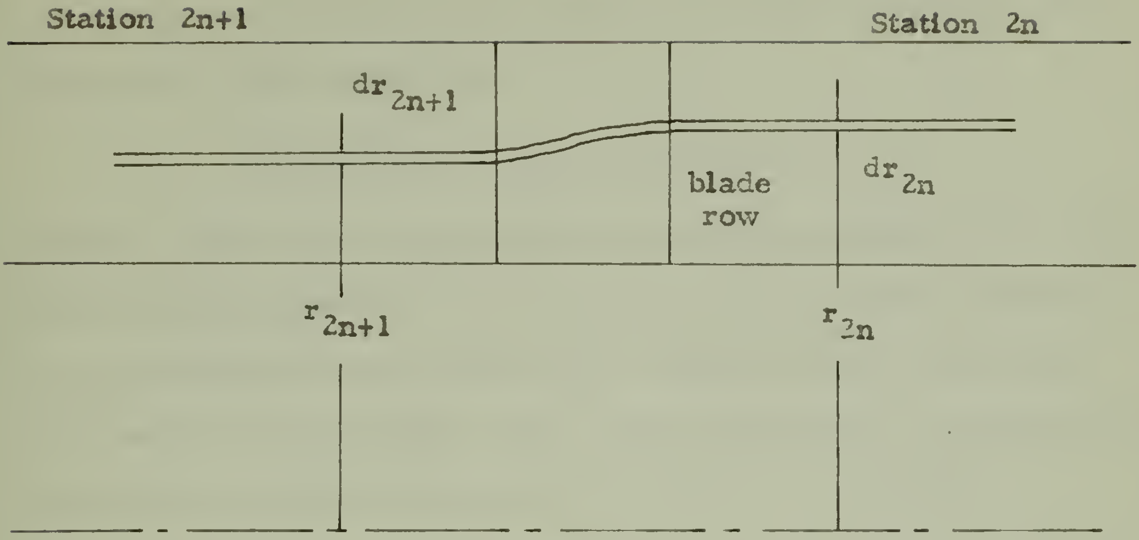

Figure 2.

$$\frac{2p_{2n}}{\rho} + w_{u_{2n}}^2 + c_{a_{2n}}^2 - \omega^2 r_{2n}^2 = \frac{2p_{2n+1}}{\rho} + w_{u_{2n+1}}^2 + c_{a_{2n+1}}^2 - \omega^2 r_{2n+1}^2 . \qquad (14)$$

The equations for the pressure gradient in the radial direction are

$$\frac{dp_{2n}}{dr_{2n}} = \rho \frac{c_{u_{2n}}^2}{r_{2n}} \qquad \text{and} \qquad \frac{dp_{2n+1}}{dr_{2n+1}} = \rho \frac{c_{u_{2n+1}}^2}{r_{2n+1}} . \qquad (15)$$

By using (15) to eliminate the pressure terms, equations (13) and (14) become, respectively,

$$\left[\frac{c_{u_{2n}}^2}{r_{2n}} + \frac{1}{2}\frac{d}{dr_{2n}}\left(c_{u_{2n}}^2 + c_{a_{2n}}^2\right)\right] dr_{2n} =$$

$$\left[\frac{c_{u_{2n+1}}^2}{r_{2n+1}} + \frac{1}{2}\frac{d}{dr_{2n+1}}\left(c_{u_{2n+1}}^2 + c_{a_{2n+1}}^2\right)\right] dr_{2n+1} , \qquad (16)$$

$$\left[\frac{c_{u_{2n}}^2}{r_{2n}} + \frac{1}{2}\frac{d}{dr_{2n}}\left(w_{u_{2n}}^2 + c_{a_{2n}}^2 - \omega^2 r_{2n}^2\right)\right] dr_{2n} =$$

$$\left[\frac{c_{u_{2n+1}}^2}{2_{2n+1}} + \frac{1}{2}\frac{d}{dr_{2n+1}}\left(w_{u_{2n+1}}^2 + c_{a_{2n+1}}^2 - \omega^2 r_{2n+1}^2\right)\right] dr_{2n+1} . \qquad (17)$$

Considering a cylindrical stream tube, the continuity equation can be written in the differential form

$$c_{a_{2n}} r_{2n} dr_{2n} = c_{a_{2n+1}} r_{2n+1} dr_{2n+1} .$$

Within the scope of the assumptions previously mentioned, these equations are quite general. It is now assumed that the leaving angles of both stator and rotor are constant with respect to flow rate and give vortex flow at the design flow rate. Thus, evaluating the leaving angles at the design condition, indicated by subscript d, we obtain

$$c_{u_{2n+1}}\Big]_d = c_{a_{2n+1}}\Big]_d \tan\gamma_1 = \frac{\alpha}{r_{2n+1}} , \qquad (18)$$

or, in the non-dimensional notation,

$$\tan\gamma_1 = \frac{\alpha}{\phi_d \xi_{2n+1}} = \frac{\psi_d}{2\phi_d} \frac{1}{\xi_{2n+1}} . \qquad (19)$$

Similarly, we obtain for the rotor leaving angle

$$\tan\beta_2 = \frac{\xi_{2n}}{\phi_d} . \qquad (20)$$

With the leaving angles so specified and the following definitions,

$$a = \frac{\psi_d}{2\phi_d} \qquad \text{and} \qquad b = \phi_d ,$$

the equation for the flow through the stator becomes

$$\left(1 + \frac{a^2}{\xi_{2n+1}^2}\right) \frac{d\phi_{2n+1}}{d\xi_{2n+1}} = \frac{\xi_{2n+1}}{\xi_{2n}} \left\{ \left[1 - \frac{\xi_{2n}^2 b}{b^2+\xi_{2n}^2} \frac{1}{\phi_{2n}}\right] \cdot \left[\frac{d}{d\xi_{2n}} \left(\frac{b^2+\xi_{2n}^2}{b^2} \phi_{2n}\right) - \frac{2\xi_{2n}}{b}\right] + \frac{2\xi_{2n} b^2}{b^2+\xi_{2n}^2} \left(\frac{1}{\phi_{2n}} - \frac{1}{b}\right) \right\} .$$

The equation for flow through a rotor row becomes

$$\frac{d}{d\xi_{2n}}\left[\frac{b^2+\xi_{2n}^2}{b^2}\,\phi_{2n}\right] - \frac{2\xi_{2n}}{b} = \frac{\xi_{2n}}{\xi_{2n-1}}\left\{\left[1+\frac{a\xi_{2n-1}^2}{a^2+\xi_{2n-1}^2}\,\frac{1}{\phi_{2n-1}}\right]\left[1+\frac{a^2}{\xi_{2n-1}^2}\right]\frac{d\phi_{2n-1}}{d\xi_{2n-1}}\right\}. \qquad (22)$$

The continuity relations are

$$\phi_{2n-1}\xi_{2n-1}d\xi_{2n-1} = \phi_{2n}\xi_{2n}d\xi_{2n} = \phi_{2n+1}\xi_{2n+1}d\xi_{2n+1}. \qquad (23)$$

The two pairs of non-linear equations (21) and (22), and (23) can be solved approximately for ϕ_m as a function of ξ_m for $m = 0, 1, 2, \ldots$ in succession.

Notice the particularly simple solution $\phi_m = \phi_d$ for all values of m. It follows that there is no streamline shift and no radial velocity in this case, and the analysis of the flow reduces to the two-dimensional one previously considered. It is largely because of this analytical simplification that the free vortex design has been used so frequently. However, for off-design flow rates, no such simple solution exists, even for the free vortex design.

To illustrate the method of solution to these equations, let us consider an off-design constant axial flow ϕ_o approaching the first stator. In this case, care must be taken in applying equation (21), since the assumption of a whirl velocity is incorporated in the right-hand side of this relation. For this incoming flow, equation (13) becomes

$$\frac{2p_1}{\rho} + c_{a_1}^2 + c_{u_1}^2 = \frac{2p_o}{\rho} + c_{a_o}^2 = \text{constant.}$$

Since $dp_o/dr_o = 0$, equation (16) becomes

$$\frac{c_{u_1}^2}{r_1} + \frac{d}{dr}\left(c_{u_1}^2 + c_{a_1}^2\right) = 0\,.$$

Substituting from equation (19), the velocity diagram relations, and the definition of a, the equation corresponding to equation (21) is

$$\left(1 + \frac{a^2}{\xi_1^2}\right) \frac{d\phi_1}{d\xi_1} = 0$$

or

$$\phi_1 = \text{constant.}$$

This constant is then determined by integrating the continuity relation from the hub to the tip.

$$\int_{\xi_i}^{1} \phi_1 \xi_1 d\xi_1 = \int_{\xi_i}^{1} \phi_o \xi_o d\xi_o$$

$$\phi_1 \tfrac{1}{2}(1 - \xi_i^2) = \phi_o \tfrac{1}{2}(1 - \xi_i^2)$$

or

$$\phi_1 = \phi_o \quad .$$

Equations (21) and (22) are applicable to all of the other blade rows now. The relation for ϕ_2 becomes, using equation (22),

$$\frac{d}{d\xi_2}\left[\frac{b^2 + \xi_2^2}{b^2}\right] - \frac{2\xi_2}{b} = 0 \, .$$

Integrating, we obtain

$$\phi_2 = b \frac{K + \xi_2^2}{b^2 + \xi_2^2}$$

where K is determined as before by integrating the continuity expression.

The flow coefficients for the following blade rows are obtained in the same manner; however, the integration for these must be done numerically. Also, another mathematical difficulty arises in the solution for ϕ_3 and the remaining stages. The existence of both independent

variables on the right-hand side of both (21) and (22) will require an iteration process. The procedure is to first let $\xi_{2n+1} = \xi_{2n}$ and solve for ϕ_{2n+1}. The continuity relation can now be integrated from ξ_i to ξ, and a relation between ξ_{2n+1} and ξ_{2n} obtained. Substitution of this relation into the differential equation for ϕ_{2n+1} yields a refined value for ϕ_{2n+1}. Fortunately, the correction to the flow coefficient is not large, and the iteration process is generally not necessary.

III. APPLICATION OF THE THREE-DIMENSIONAL THEORY

The calculation of the flow field as it progresses down the compressor was carried out for two off-design conditions. The blades were chosen such that $\phi_d = 0.57751$ and $\psi_d = 0.70000$. The average flow rate for the off-design conditions was taken as $\phi = .46000$ and $\psi = .69000$. Figures 3 through 6 show the variation of the flow coefficient versus dimensionless radius at various stations in the compressor. The flow field at lower than design flow rate is converging fairly rapidly to a steady-state condition, while at the higher flow rate the convergence does not appear to be as good.

The error in choosing $\xi_{2n+1} = \xi_{2n}$ as a first approximation is shown in Figure 7. The calculation was carried out for the fourth rotor row. An error of only approximately 2 percent of ϕ_8 at the mid-height of the blade is introduced by the first approximation. It is felt that real fluid effects will be greater than this amount.

The local values of ψ for the two off-design flow rates are shown in Figure 8. Notice that ψ is very nearly independent of the radius, agreeing with our assumptions leading to equation (10).

In standard compressors there exists a perturbation solution to the three-dimensional equations. There it is assumed that the flow ϕ_1 from a stator is approximately equal to the flow ϕ_2 from a rotor. Thus the procedure is to find a solution for which $|\phi_2 - \phi_1| \ll (\phi_2 + \phi_1)$. To the zeroth order, this results in a linear compressor performance curve in the form

$$\psi = A - B\phi \quad . \qquad (24)$$

The two-dimensional theory also produced an equation of this type, since in that case ϕ_1 was taken identically equal to ϕ_2.

To examine the possibilities of this approach for the proposed helium compressor, consider the approximate performance equation

$$\psi = 2[\xi^2 + \xi\phi_1\tan\gamma_1 - \xi\phi_2\tan\beta_2] \ . \tag{25}$$

For free vortex blading, equation (25) becomes

$$\psi = 2 \quad \frac{\psi_d}{2\phi_d}\phi_1 - \frac{\xi^2}{\phi_d}\phi_2 + \xi^2 \qquad . \tag{26}$$

If we now assume

$$\phi_1 = \tfrac{1}{2}(\phi_1+\phi_2) + \tfrac{1}{2}(\phi_1-\phi_2) = \phi_o + \Delta\phi \tag{27a}$$

and

$$\phi_2 = \tfrac{1}{2}(\phi_1+\phi_2) - \tfrac{1}{2}(\phi_1-\phi_2) = \phi_o - \Delta\phi \ , \tag{27b}$$

then equation (26) can be written

$$\psi = 2\xi^2 + \frac{\phi_o}{\phi_d}[\psi_d - 2\xi^2] + \frac{\Delta\phi}{\phi_d}[\psi_d + 2\xi^2] \ . \tag{28}$$

Typical values of ψ_d and $\Delta\phi$ for a conventional compressor allow the term containing $\Delta\phi$ to be ignored. However, for the compressor proposed in this report, ψ_d is approaching $2\xi^2$ at the hub, and the term containing $\Delta\phi$ can no longer be neglected. Figure 9 shows the performance curves of both types of compressors with and without the inclusion of the $\Delta\phi$ term. The inadequacy of the two-dimensional solution in the case of the helium compressor is obvious. To the scale of the graph, no difference can be observed for the conventional compressor.

Figure 10 shows the total pressure variation along the blades after the flow has essentially settled into a steady pattern. For lower

than design flow rates, more work is being done by the tips, while at higher flow rates, the roots give the greater rise. The cumulative difference after six stages is still less than half the design pressure rise for a single stage.

It was mentioned previously that it is desirable to have

$$\frac{w_1^2 - w_2^2}{w_1^2} < 0.6 .$$

This quantity is plotted in Figure 11. Possible difficulties are indicated at lower than design flow rates. A higher hub ratio would eliminate this difficulty. The corresponding ratio for the stator is plotted in Figure 12. Since the stators are in a field of decreasing pressure, no difficulties are expected here.

The off-design entering angles for the stator and rotor are plotted in Figures 13 and 14, respectively. The stators are very critical and will require care in their design. Sharp leading edges of the stators would probably cause high losses. The off-design flow incidence angle deviations for the rotors appear satisfactory.

IV. CONCLUDING REMARKS

It has been demonstrated that high reaction blading can be used in multi-stage axial compressors to produce a significant increase in pressure rise per stage over conventional blading. This type of blading could be used in a closed-cycle helium compressor and greatly reduce the total number of stages required. The analysis also indicates that a hub ratio greater than 0.6 would possibly be a more efficient design, since stator incidence flow angle deviations become quite large near the hub in the example shown.

It was also shown that the usual linearization of the three-dimensional equations of flow is not valid for this type of blading. However, a numerical solution allowing for the shift of the streamlines does converge to a steady, repeating flow pattern after the first five or six stages for flows as much as twenty per cent off design.

REFERENCES FOR PART I

1. Johnson, I. A. and Bullick, R. O., Editors, "Aerodynamic Design of Axial-Flow Compressors," NACA RM E56B03 (1956).

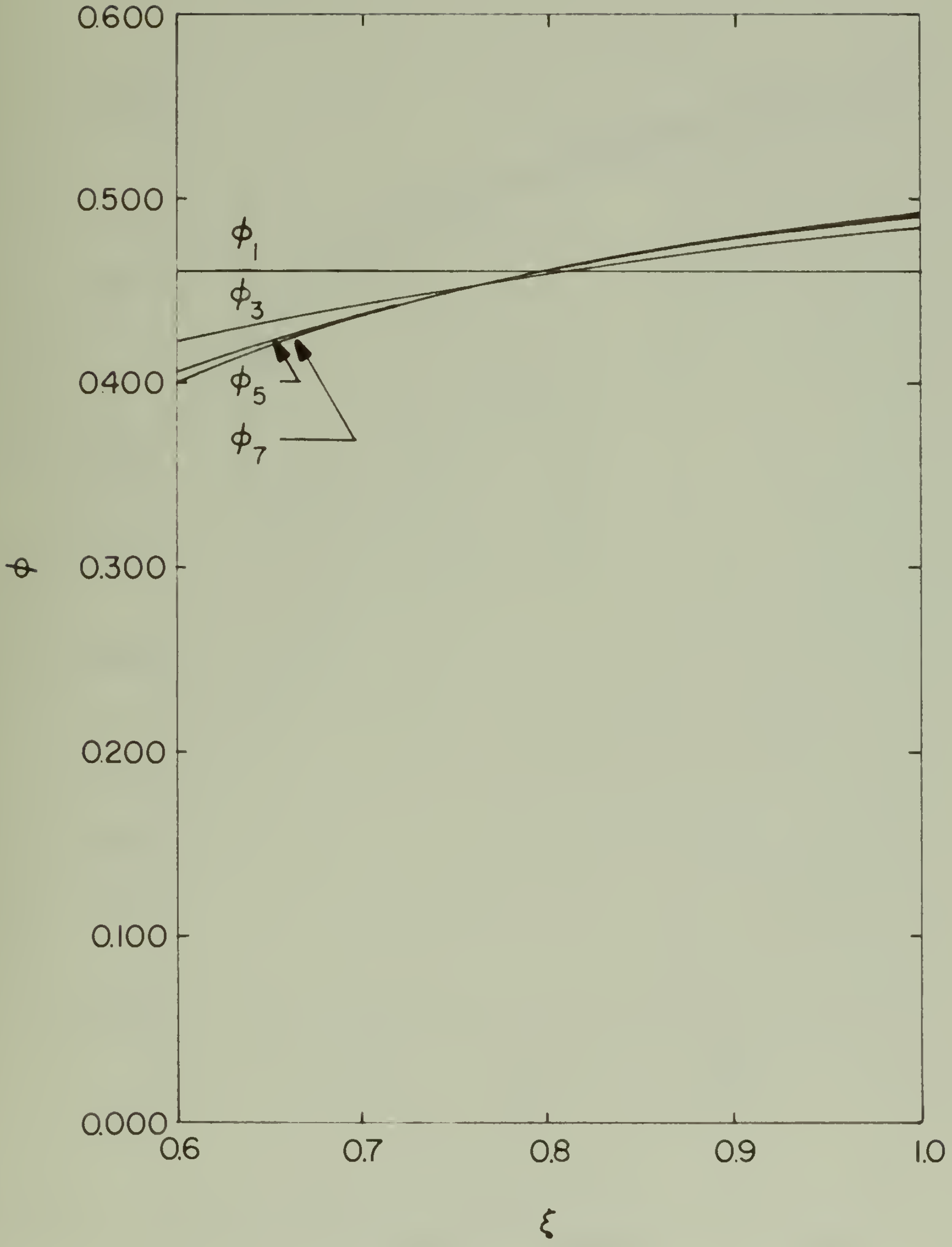

Figure 3. Stator Axial Velocity Coefficients, $\overline{\Phi}$ = .46000 .

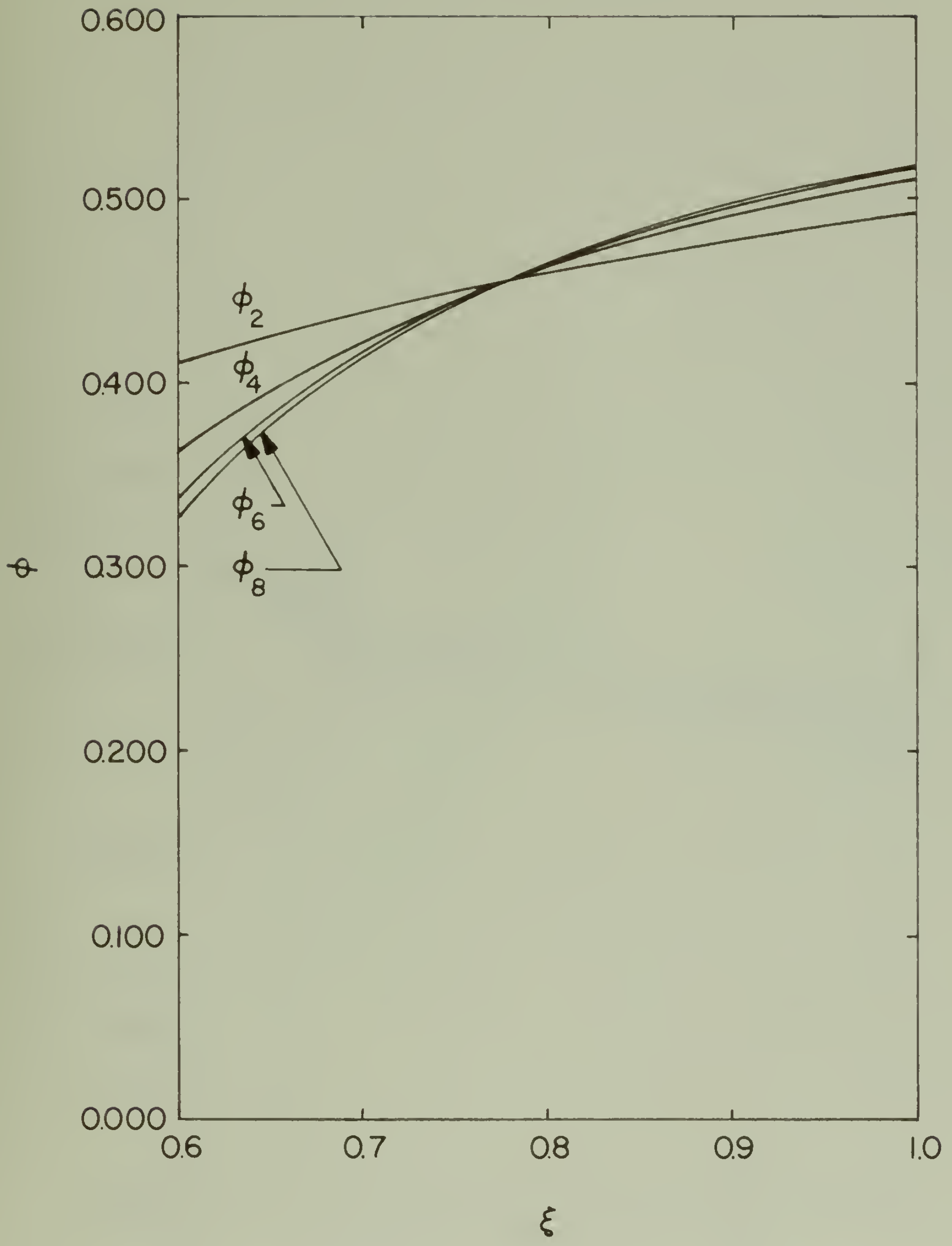

Figure 4. Rotor Axial Velocity Coefficients, $\overline{\phi} = .46000$.

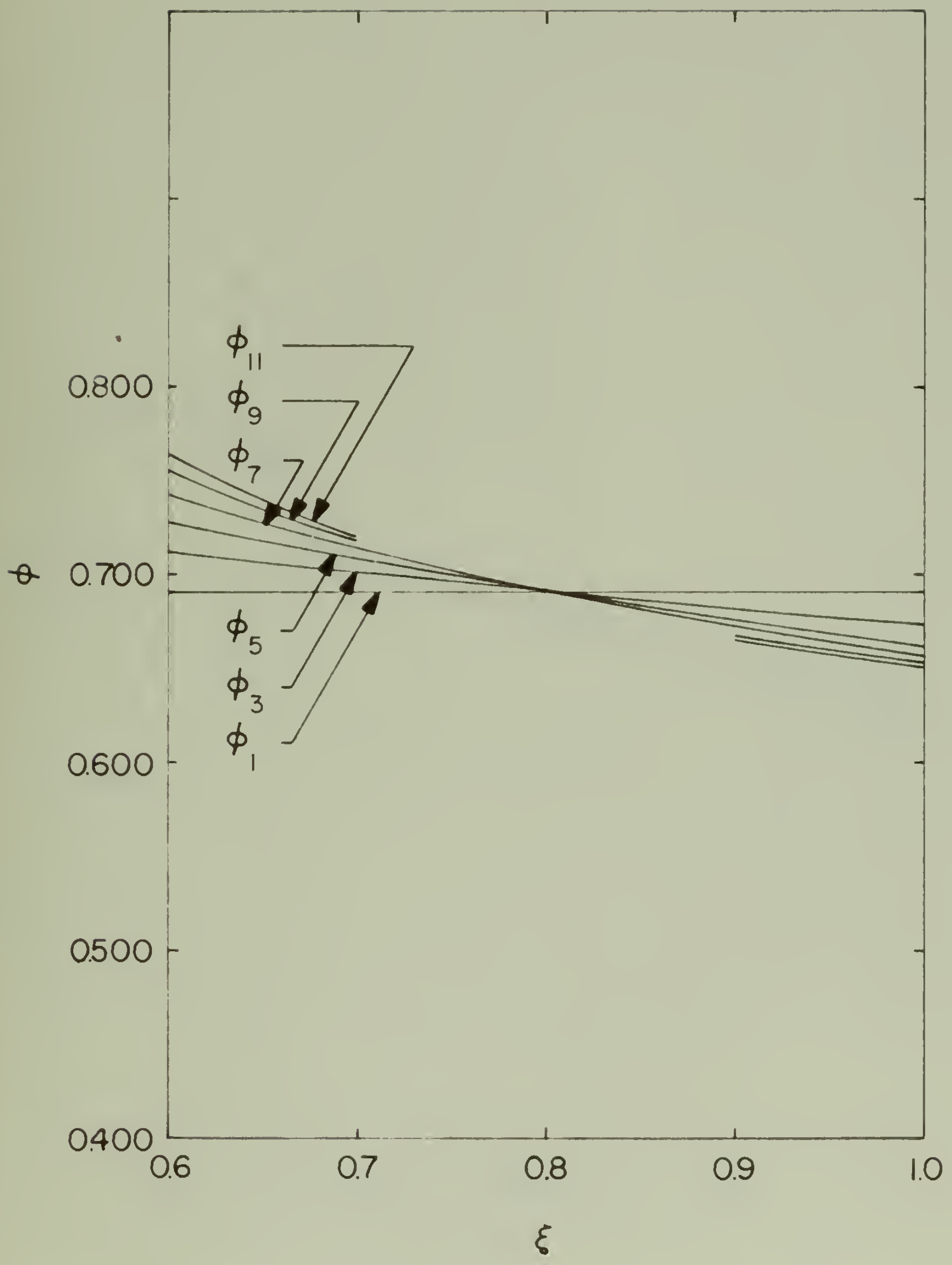

Figure 5. Stator Axial Velocity Coefficients, $\overline{\phi} = .69000$.

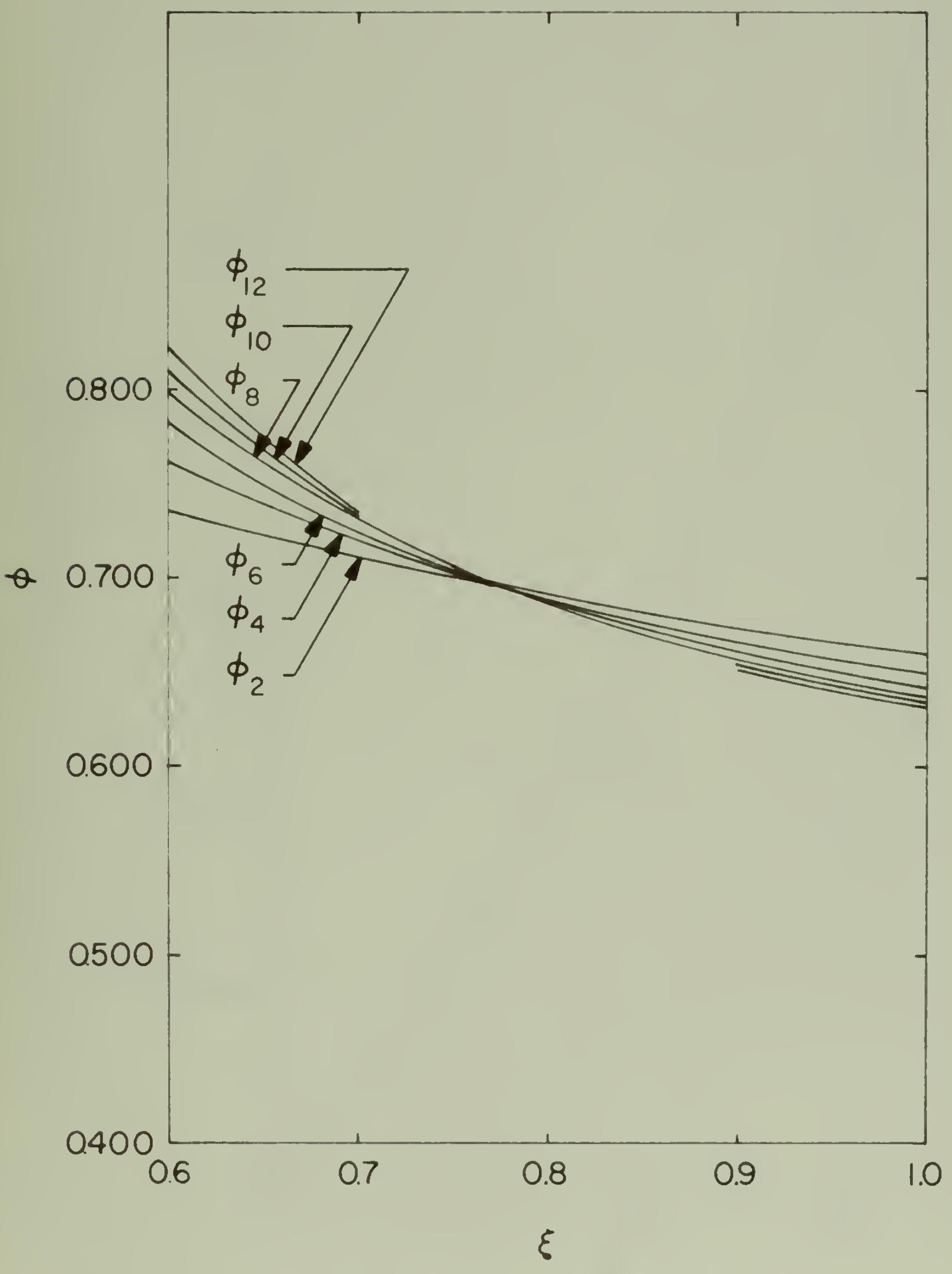

Figure 6. Rotor Axial Velocity Coefficients, $\overline{\phi} = .69000$.

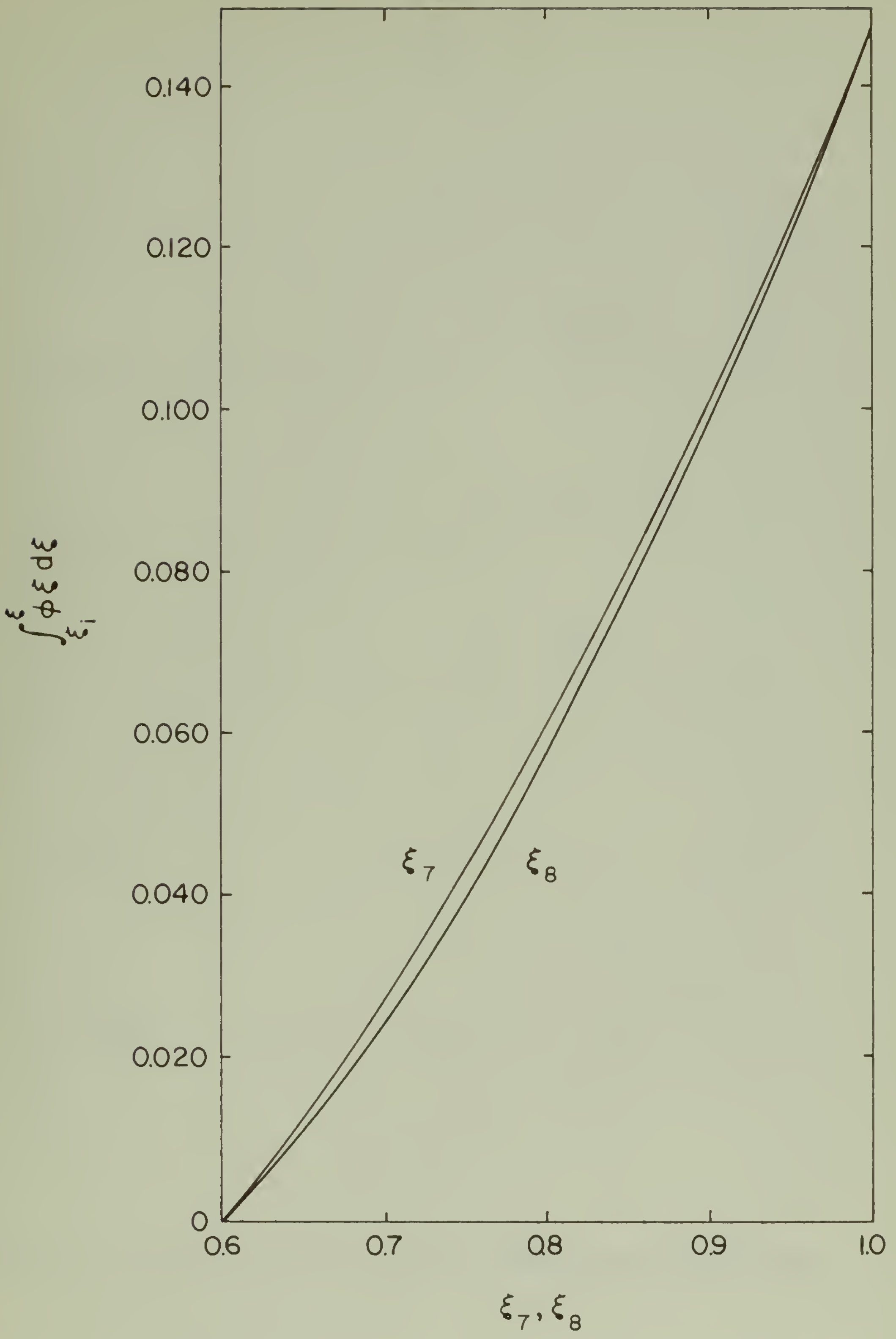

Figure 7. Streamline Radii Upstream and Downstream of a Rotor.

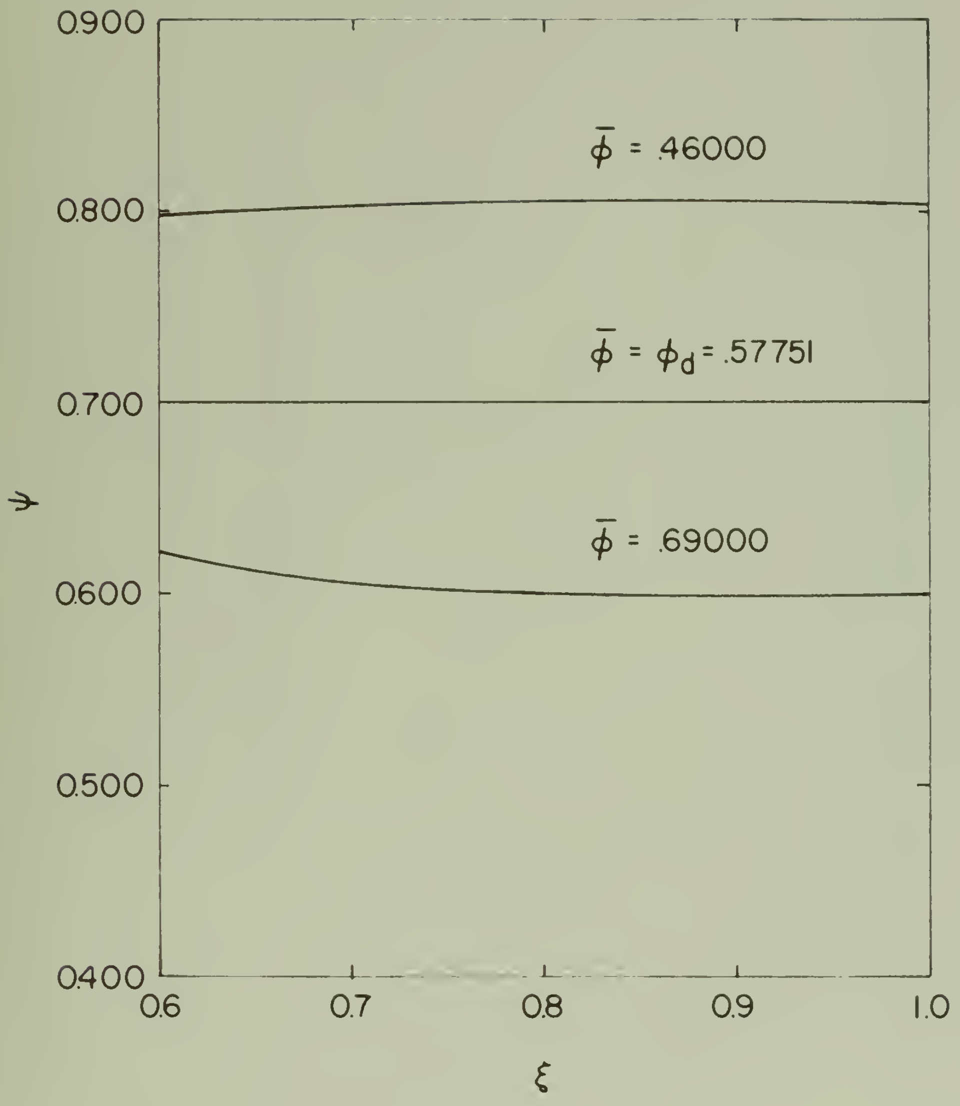

Figure 8. Local Value of ψ Versus Non-Dimensional Radius.

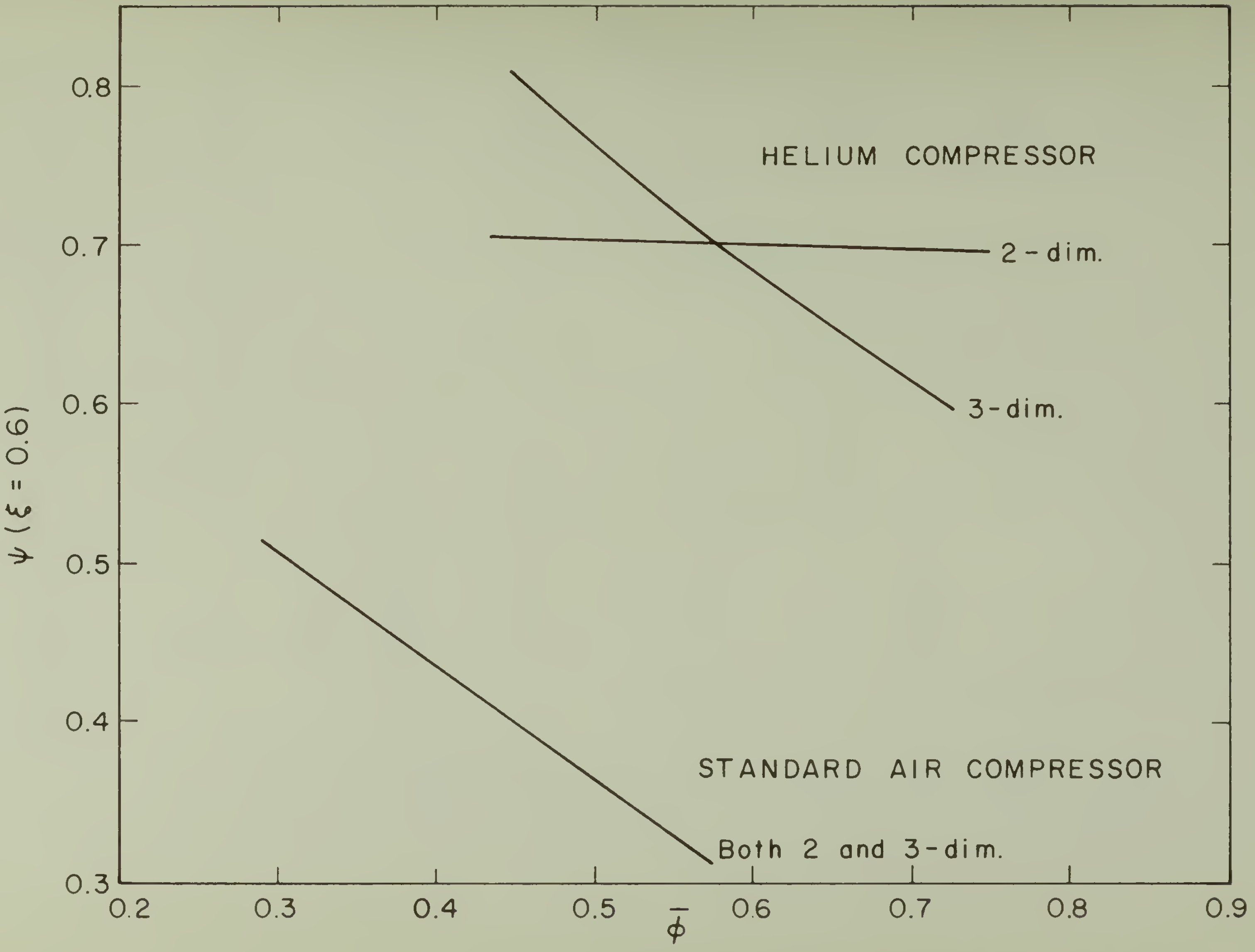

Figure 9. Effect of Two-Dimensional Linearization on Performance Curves.

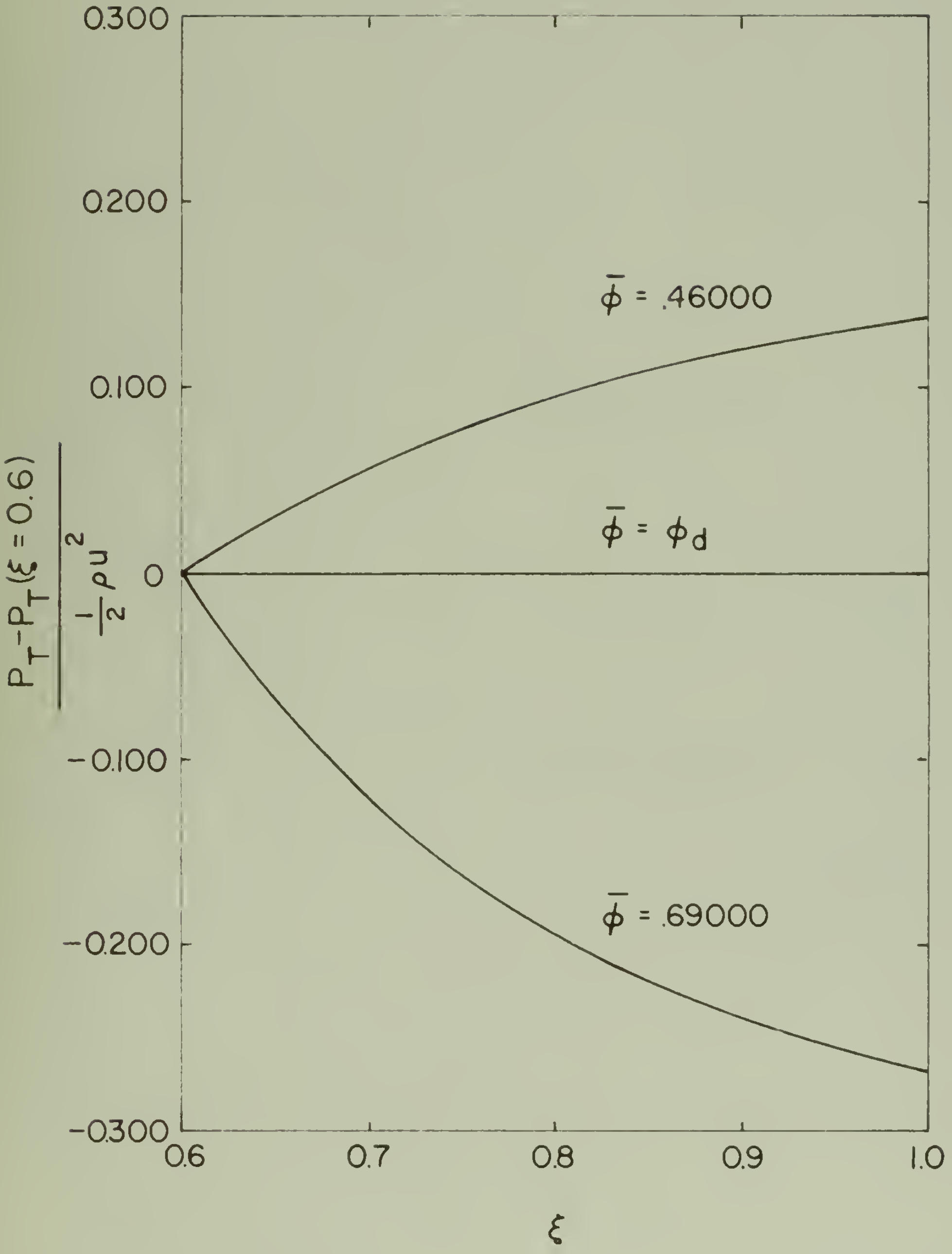

Figure 10. Total Pressure Variation with Radius.

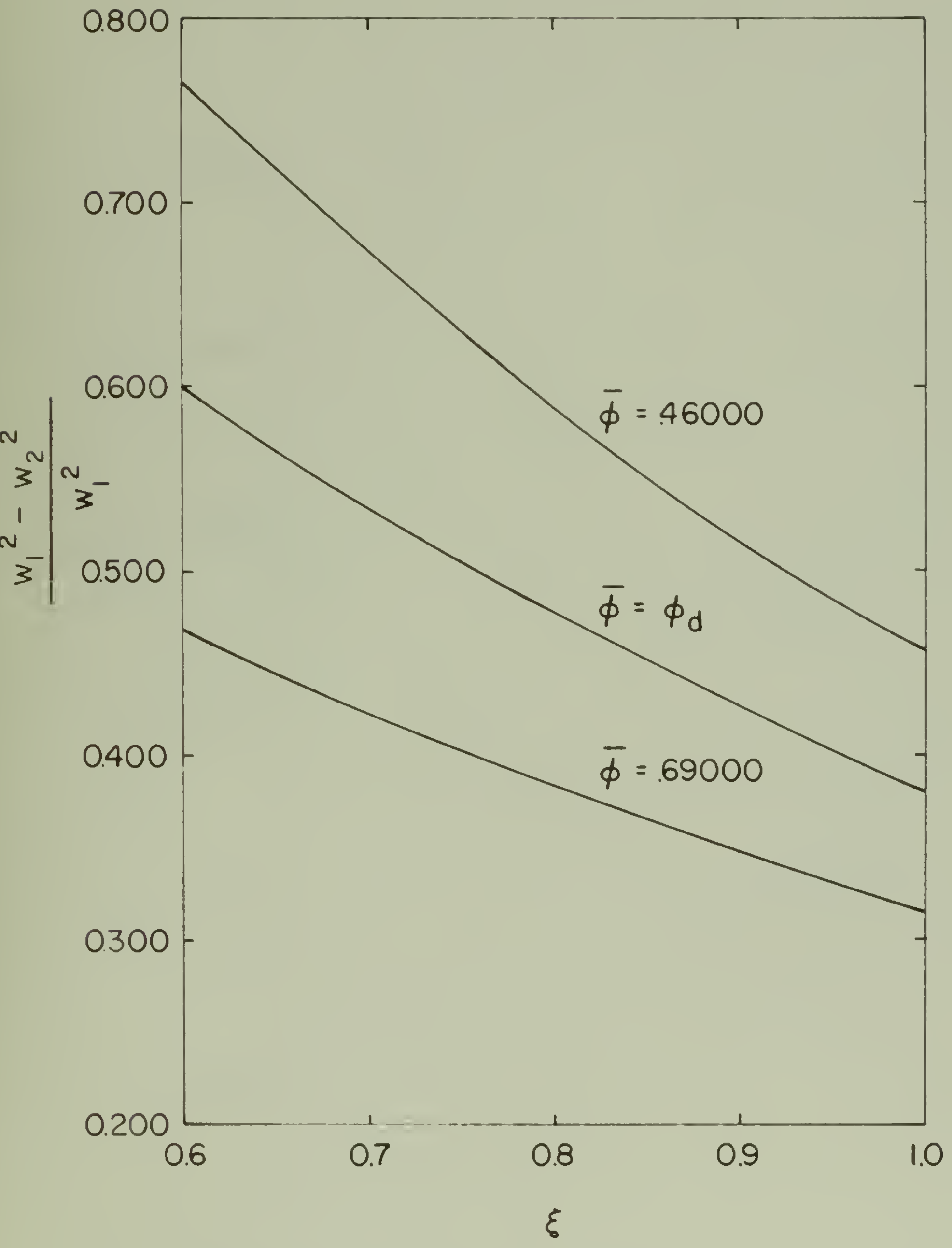

Figure 11. Kinetic Energy Conversion Through the Rotor Versus Radius.

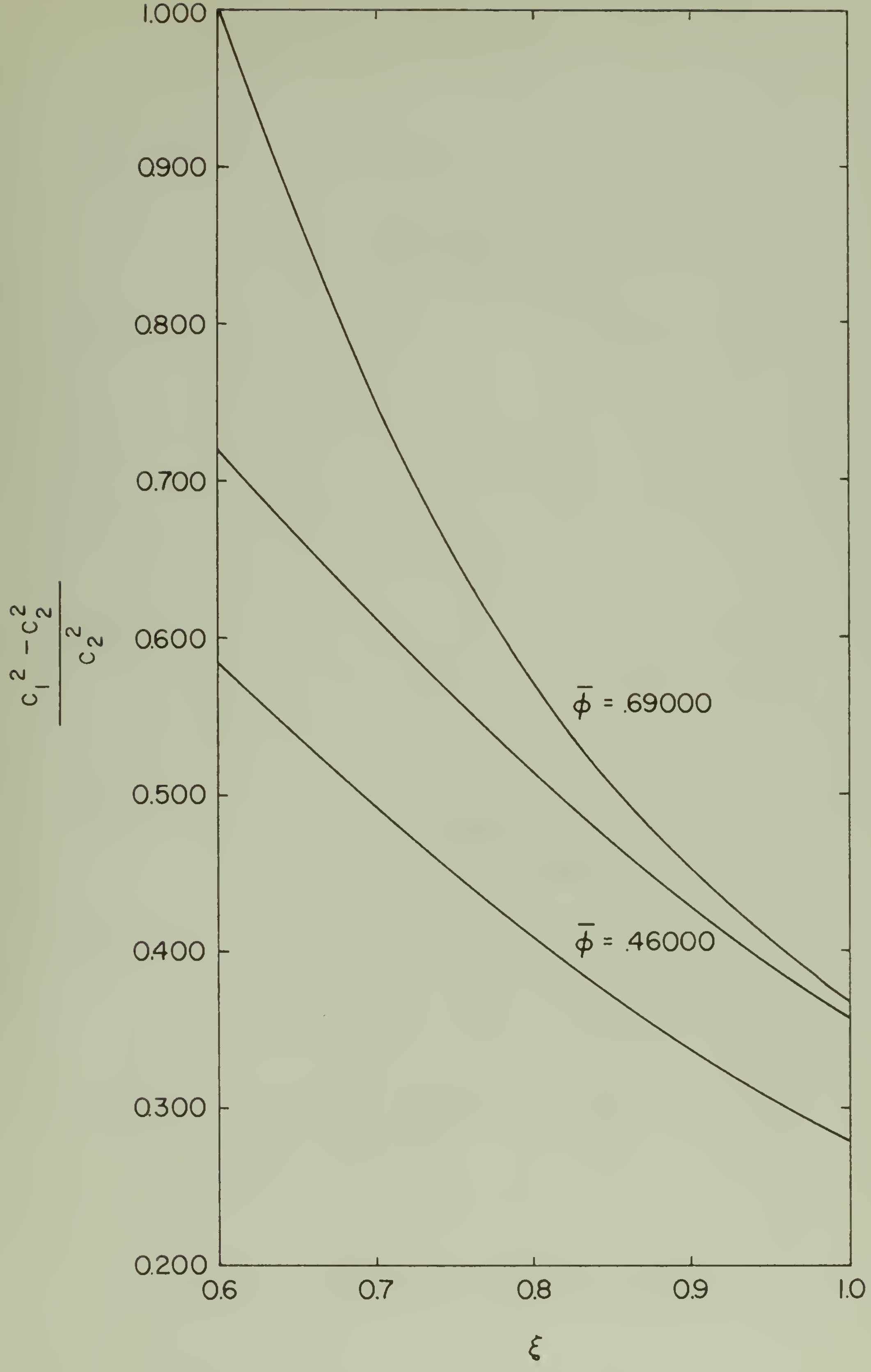

Figure 12. Kinetic Energy Conversion Through the Stator Versus Radius.

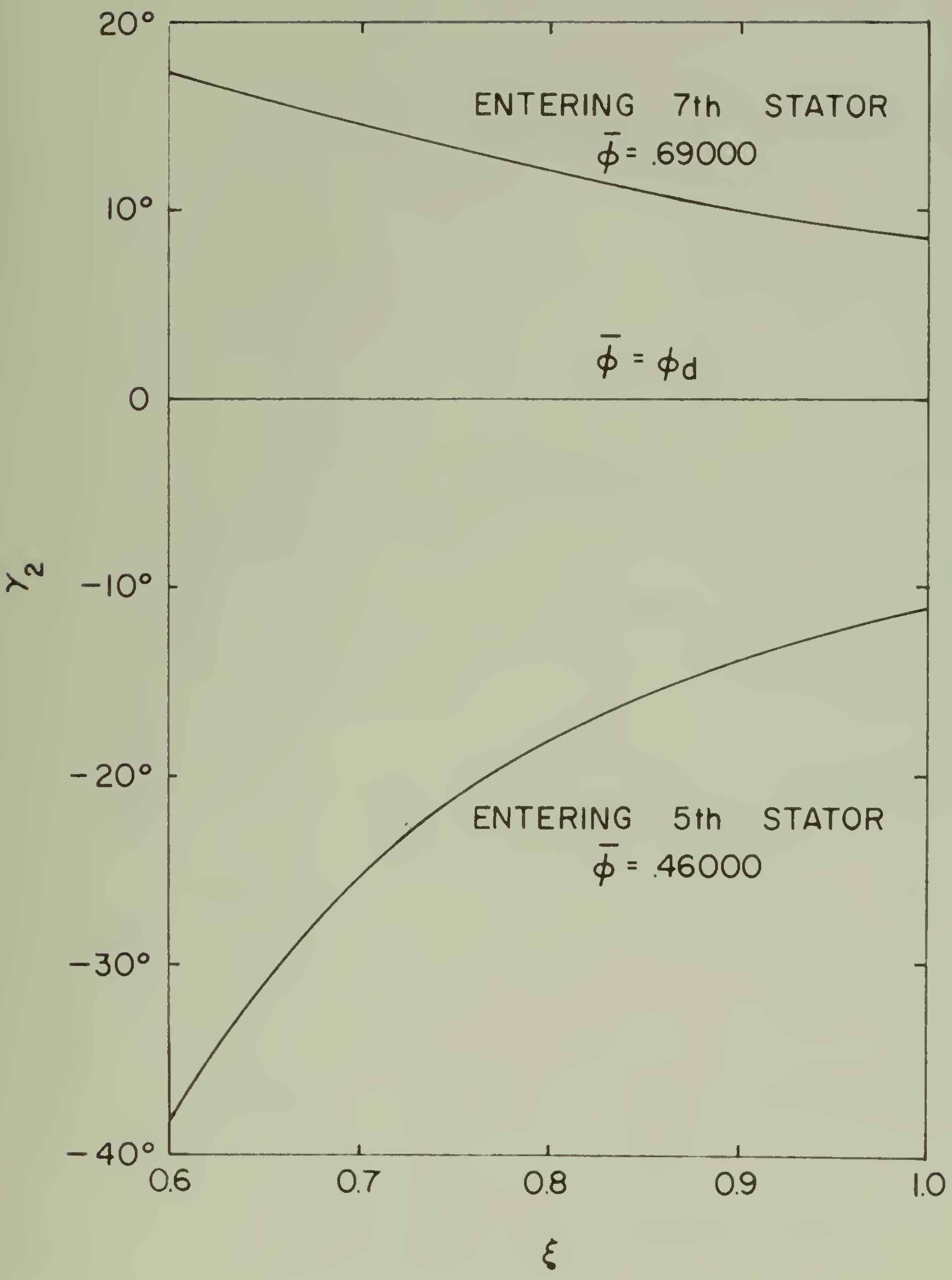

Figure 13. Stator Flow Entering Angles.

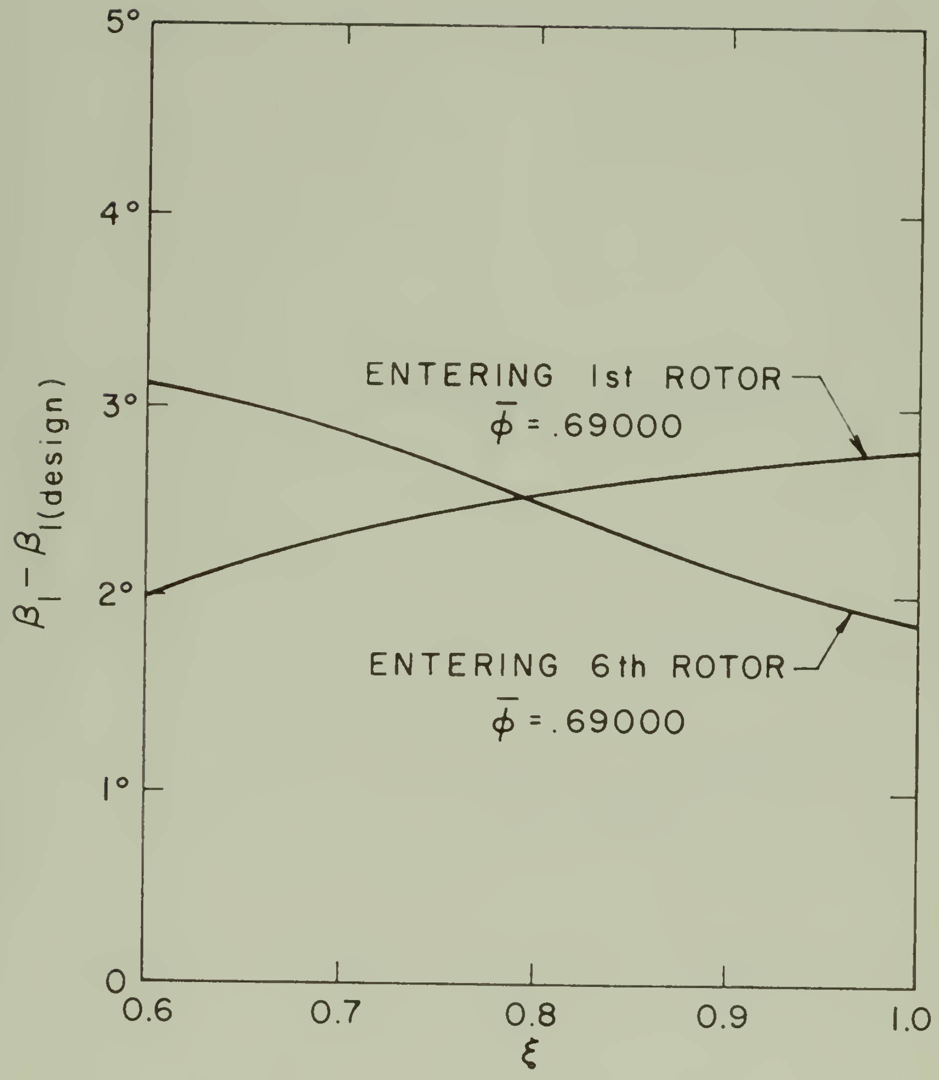

Figure 14. Rotor Flow Engering Angles.

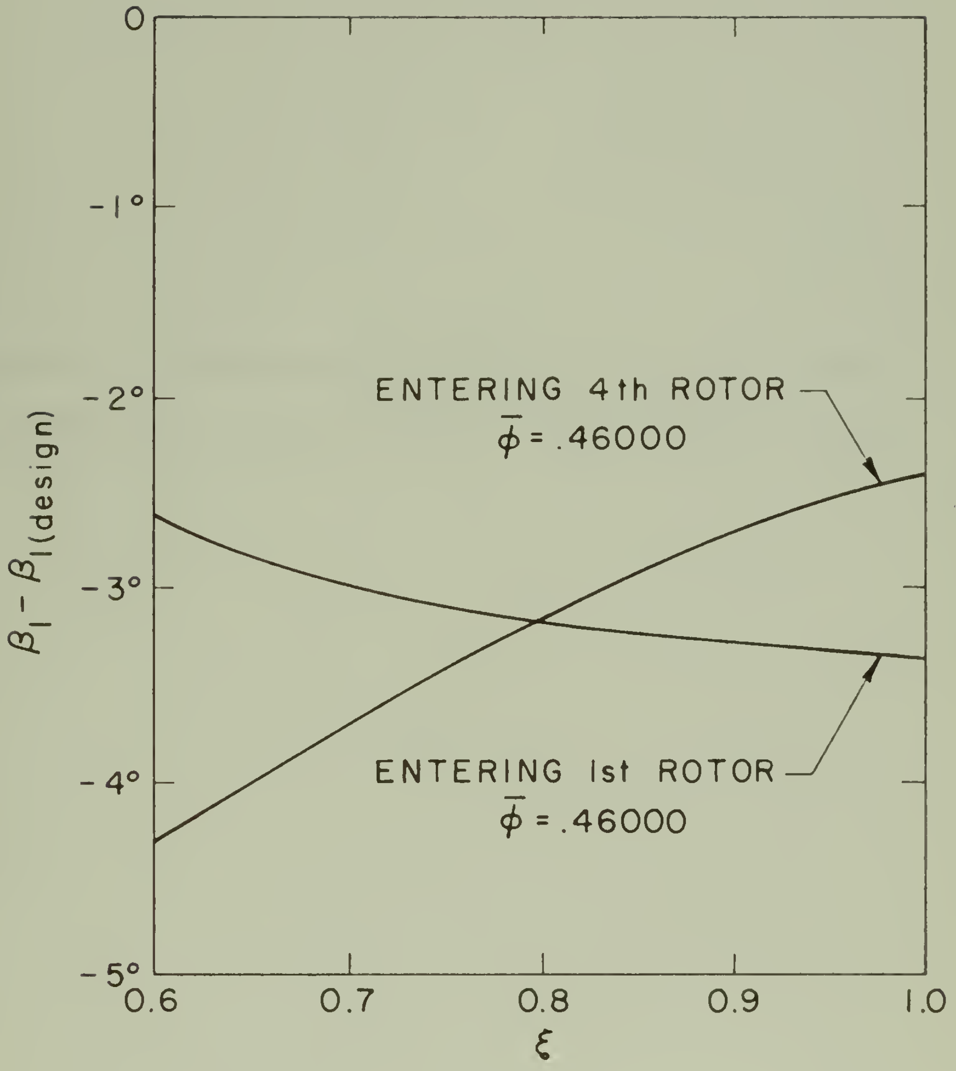

Figure 14 (continued). Rotor Flow Entering Angles.

PART II. A DESIGN STUDY OF A MULTI-STAGE AXIAL COMPRESSOR WITH BLADING OF HIGH ASPECT RATIO

ABSTRACT FOR PART II

A method for designing blades of high aspect ratio in a multistage axial compressor is investigated. This method requires a calculation of the flow induced by all blade rows. The method is illustrated for the limiting condition of hub ratio equal to unity and then is carried out for the more realistic case of finite hub ratio.

An example of a blade design for a particular flow is carried out. The results are compared with those of a previous design for the same flow conditions but based on a theory applicable for blading of low aspect ratio.

SUMMARY FOR PART II

The flow through most present-day axial flow compressors is frequently analyzed by applying a three-dimensional theory that is based on the assumption of blading with low aspect ratio. Even though existing compressors do not have what could be called low aspect ratio blades, the theory predictions and experimental results show reasonable agreement.

Where weight considerations are of primary concern, the possibility of reducing the size of a compressor by shortening its length is attractive. There is no known reason why the blade rows cannot be held to their same height but shortened in chord. There is, however, a difficulty in applying the aforementioned analysis. There, it is assumed that equilibrium flow patterns exist at the leading and trailing edges of the blades. THis is identical to assuming low aspect ratio for the blades, since they must be wide enough to allow all changes in the flow to occur entirely within the blade row itself. Several extensions of the theory have been developed to take account of the non-equilibrium flow near the blade rows. Some of these analyses assumed small vorticity throughout the flow field and also a small change in vorticity through the blade rows. Another theory relaxed the restriction of small vorticity throughout the flow field.

The theory presented in this thesis is an extension of the latter approach, and is based on the assumptions of closely spaced blades of high aspect ratio. The equations of motion are linearized by a perturbation scheme that assumes small changes in perturbation velocities across the blade rows. To illustrate the method, the calculation is first

restricted to the limiting case of hub ratio close to unity. Then the more involved problem for any hub ratio is investigated. An example is worked for blades of aspect ratio about three. Here, there appeared little difference between the theory applicable to blades of low aspect ratio and the theory of blades of low aspect ratio.

I. INTRODUCTION

The theory of three-dimensional flow in the axial compressor described in Part I of this thesis is concerned only with flow conditions far upstream and far downstream of a blade row. This theory would be applicable to blades of very low aspect ratio. The difference between these velocity profiles and the actual profiles near the leading and trailing edges of the blades was assumed to be negligible. It was on this basis that the entering flow angles for the blades were determined. If the aspect ratio is not very low, it is possible to obtain more exact information about the flow pattern near the blade rows by making use of some of Marble's results (Ref. 1). This has been done by Bowen, Sabersky, and Rannie in Ref. 2. The method carried out by these investigators forms the basis of the theory to be discussed in this report. The approach is to consider the disturbances due to rows of blades of high aspect ratio placed very close together. Here, the flow in any particular blade row is influenced by neighboring blade rows. In the three-dimensional theory of Part I, the changes in the flow pattern were assumed to occur entirely within the blade row itself and one blade row did not affect its neighbor.

The analysis begins with the calculation of the disturbances due to an infinitesimally thin disk. These disturbances can then be superimposed to form a blade with finite axial extent. The effect of many blade rows can be determined by the superposition of the disturbances due to the finite row. In this way, the flow pattern for a multi-stage axial turbomachine can be constructed. For a repeating flow pattern, the summation of the effects of all blade rows is possible.

II. TWO-DIMENSIONAL THEORY

A. Equations and Boundary Conditions

Before proceeding directly into the three-dimensional theory of high aspect ratio blading, it is informative to investigate first the limiting case of high hub ratio. This problem is simpler because the radial pressure gradients vanish far from the blade. The analysis is based upon the disturbances due to a disk at $x = 0$ (see Figure 1), and the equations of motion are written subject to several assumed conditions.

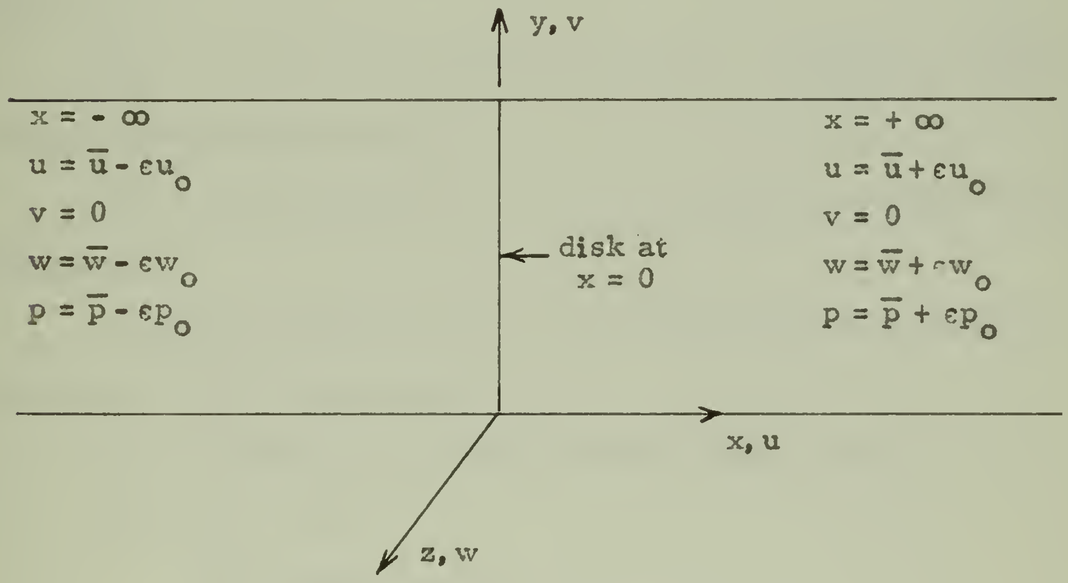
y, v
$x = -\infty$
$u = \bar{u} - \epsilon u_o$
$v = 0$
$w = \bar{w} - \epsilon w_o$
$p = \bar{p} - \epsilon p_o$
disk at
$x = 0$
$x = +\infty$
$u = \bar{u} + \epsilon u_o$
$v = 0$
$w = \bar{w} + \epsilon w_o$
$p = \bar{p} + \epsilon p_o$
x, u
z, w

Figure 1

These assumptions are: (1) there are no circumferential variations; that is, $\frac{\partial}{\partial z}(\ ) = 0$. This is equivalent to having a disk with an infinite number of blades. (2) The flow is incompressible, the density ρ being

held constant. The continuity and momentum equations then become

$$\frac{\partial u}{\partial x} + \frac{\partial v}{\partial y} = 0 \tag{1}$$

$$u\frac{\partial u}{\partial x} + v\frac{\partial u}{\partial y} = -\frac{1}{\rho}\frac{\partial p}{\partial x} \tag{2}$$

$$u\frac{\partial v}{\partial x} + v\frac{\partial v}{\partial y} = -\frac{1}{\rho}\frac{\partial p}{\partial y} \tag{3}$$

$$u\frac{\partial w}{\partial x} + v\frac{\partial w}{\partial y} = 0 \tag{4}$$

where u, v, and w are the gas velocity components in the x, y, and z directions, and p is the static pressure.

The boundary conditions to be imposed on this system are as follows:

(1) $v = 0$ at $y = 0$ and $y = b$ for all x, since the walls of the compressor are streamlines.

(2) u is continuous at $x = 0$ from continuity through the actuating disk.

(3) v is continuous at $x = 0$ due to the component of force being zero in the y direction.

(4) w is allowed to change discontinuously across $x = 0$.

(5) At $x = -\infty$,

$u = \overline{u}(y) - \epsilon u_o(y)$,

$v = 0$,

$w = \overline{w}(y) - \epsilon w_o(y)$,

$p = \overline{p} - \epsilon p_o =$ constant.

(6) At $x = +\infty$,

$u = \overline{u}(y) + \epsilon u_o(y)$,

$v = 0$,

$$w = \overline{w}(y) + \epsilon w_o(y) ,$$

$$p = \overline{p} + \epsilon p_o = \text{constant.}$$

These last two boundary conditions are written in a form so as to conform with the following perturbation scheme. Far upstream and far downstream of the disk, the flow is independent of x ; any disturbance due to the disk having been smoothed out. Close to the disk, the flow is disturbed by a small amount, and the following perturbations are assumed, where the symbol ϵ is carried only to denote the assumed small quantities.

$$\begin{aligned} u &= \overline{u}(y) \mp \epsilon u_o(y) + \epsilon u_1(x, y) \\ v &= \epsilon\, v_1(x, y) \\ w &= \overline{w}(y) \mp \epsilon w_o(y) + \epsilon w_1(x, y) \\ p &= \overline{p} \mp \epsilon p_o + \epsilon p_1(x, y) \end{aligned} \tag{5}$$

Notice that $\overline{p}$ and p_o are assumed independent of either x or y and that the mean value of v is zero. The top signs are for $-\infty < x < 0$ and the bottom signs are for $0 < x < +\infty$.

Introducing equation (5) into the equation of motion yields the linear set

$$\frac{\partial u_1}{\partial x} + \frac{\partial v_1}{\partial y} = 0 \tag{6}$$

$$\overline{u}\, \frac{\partial u_1}{\partial x} + \frac{\partial \overline{u}}{\partial y}\, v_1 = -\frac{1}{\rho}\, \frac{\partial p_1}{\partial x} \tag{7}$$

$$\overline{u}\, \frac{\partial v_1}{\partial x} = -\frac{1}{\rho}\, \frac{\partial p_1}{\partial y} \tag{8}$$

$$\overline{u}\, \frac{\partial w_1}{\partial x} + \frac{\partial \overline{w}}{\partial y}\, v_1 = 0 \tag{9}$$

B. Solution of the Equations for the Actuating Disk

The first three of the preceding equations (6, 7, and 8) can be combined to give the differential equation for v, as

$$\frac{\partial^2 v_1}{\partial x^2} + \frac{\partial^2 v_1}{\partial y^2} - \frac{1}{\bar{u}}\frac{\partial^2 \bar{u}}{\partial y^2} v_1 = 0 \tag{10}$$

with the boundary conditions that $v = 0$ at $y = 0$ and $y = b$. A solution to equation (10) that satisfies these boundary conditions is

$$v_1 = U \sum_{n=1}^{\infty} A_n e^{\pm \lambda_n \frac{x}{b}} Y_n(y) \tag{11}$$

where

$$U = \frac{1}{b} \int_0^b \bar{u}\, dy$$

and $Y_n(y)$ satisfies the differential equation

$$\frac{d^2 Y_n}{dy^2} + \left[\left(\frac{\lambda_n}{b}\right)^2 - \frac{\bar{u}''}{\bar{u}}\right] Y_n = 0$$

with boundary conditions

$$Y_n(o) = Y_n(b) = 0 .$$

Equation (6) then yields

$$u_1 = \mp U \sum_{n=1}^{\infty} A_n \frac{b}{\lambda_n} e^{\pm \lambda_n \frac{x}{b}} Y_n'(y) , \tag{12}$$

where the prime denotes differentiation with respect to y. Notice that the boundary conditions on u are satisfied at $x = -\infty$ and $x = +\infty$. From the continuity of u across the disk, the following relation is obtained

$$u_o(y) = - U \sum_{n=1}^{\infty} A_n \frac{b}{\lambda_n} Y_n'(y) . \tag{13}$$

Since $\overline{u}$ and u_o are to be chosen and the shape of the blades is to be determined, it is possible at this point to choose $A_n = 0$ for $n > 1$. Also, if $\overline{u}$ is chosen as a linear function of y, then

$$Y_1 = \sin \frac{\lambda_1 y}{b}$$

and

$$\lambda_1 = \pi \ .$$

Note that it is not necessary that these particular choices be made. It is done here only to reduce the amount of algebra in the rest of the analysis. It will be pointed out later that these choices can indeed represent the flow through a conventional compressor quite well. Therefore, the perturbation velocities become

$$u_1 = \pm u_o \, e^{\pm \pi \frac{x}{b}}$$

and

$$v_1 = - e^{\pm \pi \frac{x}{b}} \int_0^y u_o(\eta) \, d\eta \ .$$

Using equation (9), w_1 is determined as

$$w_1 = \pm \frac{1}{\overline{u}} \frac{d\overline{w}}{dy} e^{\pm \pi \frac{x}{b}} \int_0^y u_o(\eta) \, d\eta \ , \tag{14}$$

and with the use of equation (7),

$$\frac{1}{\rho} p_1 = \mp e^{\pm \pi \frac{x}{b}} \left[\overline{u} \, u_o - \frac{d\overline{u}}{dy} \int_0^y u_o(\eta) \, d\eta \right]. \tag{15}$$

There are several requirements that we can now impose. First, we can require the total pressure rise across the disk to be a constant. This will insure that the flow pattern will repeat itself. This is a similar condition to that set upon the work coefficient in Part I of this paper. To

calculate the change in total pressure, one needs the change in whirl and the change in static pressure. The change in whirl is

$$\Delta w = w(+o, y) - w(-o, y) ,$$

and with the use of equations (5) and (14) becomes

$$\Delta w = 2\epsilon w_o - 2\epsilon \frac{1}{\bar{u}} \frac{d\bar{w}}{dy} \int_0^y u_o(\eta)\, d\eta \ .$$

The change in static pressure is

$$\frac{\Delta p}{\rho} = \frac{p}{\rho}(+o, y) - \frac{p}{\rho}(-o, y) \ ,$$

and using equations (5) and (15), becomes

$$\frac{\Delta p}{\rho} = 2\epsilon \frac{p_o}{\rho} + 2\epsilon \left[\bar{u}\, u_o - \frac{d\bar{u}}{dy} \int_0^y u_o(\eta) d\eta \right] \ .$$

Since u and v are continuous through the disk, the change in total pressure is

$$\frac{\Delta p_T}{\rho} = \frac{\Delta p}{\rho} + \bar{w}\, \Delta w$$

or

$$\frac{\Delta p_T}{\rho} = 2\epsilon \frac{p_o}{\rho} + 2\epsilon\,(\bar{u}\, u_o + \bar{w}\, w_o) + 2\epsilon \left(\frac{d\bar{u}}{dy} + \frac{\bar{w}}{\bar{u}} \frac{d\bar{w}}{dy} \right) \int_0^y u_o(\eta) d\eta \ , \qquad (16)$$

and we require this to be constant. Thus, we now have the four unknown functions of y : $\bar{u}$, u_o, $\bar{w}$, and w_o, and two constants $\bar{p}$ and p_o with one equation (16) relating them. Also, since we are interested only in the pressure rise in a compressor, we are not immensely concerned with the mean pressure, $\bar{p}$. The pressure change across the disk is $2p_o$, and this is the more important quantity.

Another condition that we can require is that the total pressure far upstream and far downstream be constant from root to tip. Note

that this is not a necessary condition, but is a common choice in compressor design and gives two more relations connecting our four unknown functions of y. For the total pressure to be constant we must require that

$$\frac{p}{\rho} + \tfrac{1}{2}\left[(\bar{u}-\varepsilon u_o)^2 + (\bar{w}-\varepsilon w_o)^2\right] = \text{constant}$$

and (17)

$$\frac{p}{\rho} + \tfrac{1}{2}\left[(\bar{u}+\varepsilon u_o)^2 + (\bar{w}+\varepsilon w_o)^2\right] = \text{constant}$$

and since p/ρ is constant far upstream and far downstream of the disk, we derive the following two equations by adding and subtracting equations (17) and keeping only first order in ε:

$$\begin{aligned} \bar{u}^2 + \bar{w}^2 &= K_1 \\ u_o\bar{u} + w_o\bar{w} &= K_2 \end{aligned} \tag{18}$$

where K_1 and K_2 are undetermined constants.

The second condition of equations (18) is now actually the same as equation (16). If the disk were to act as a stator, then (16) would reduce to

$$-\frac{p_o}{\rho} = \bar{u}u_o + w_o\bar{w} - \left(\frac{d\bar{u}}{dy} + \frac{\bar{w}}{\bar{u}}\,\frac{d\bar{w}}{dy}\right)\int_0^y u_o(\eta)d\eta\ . \tag{19}$$

Since p_o/ρ is a constant, and from (18) $\bar{u}u_o + w_o\bar{w} = K_2$, the last term of equation (19) must be a constant. Since the integral is obviously zero at $y = 0$, then this constant must be zero. Thus, with the assumption of constant total pressure, we have four unknown functions of y and two conditions upon them. Hence, for example, we could pick u, u_o, and p_o, and the flow will be completely determined. Once this

has been done, the shape of the blades can be found.

To derive the effect on the flow due to a blade of finite width a and height b, we can sum from $x = 0$ to $x = a$ the disturbance due to a disk located at $x = \xi$ where ξ ranges from 0 to a. Notice, however, that here one must make a choice of the shape of the loading on the blade. That is, we must require that each disk contribute some fraction $f(\xi)d\xi$ of the disturbance of the blade. In the problem proposed in this report, we are at liberty to pick the function $f(\xi)$. We then go on to find the shape of the blade. However, the inverse problem of specifying the blading and then finding the flow is much more difficult. In that case, the loading function is in general a function of both x and y and depends on the entering flow angles.

C. Superposition of Actuating Disks for Multi-Stage Compressors

Given the function $f(\xi)$, we can proceed to determine the velocities u and w throughout the compressor. The function $f(\xi)$ is normalized such that

$$\int_0^a f(\xi)d\xi = 1 .$$

For a finite stator of width a, height b, and leading edge at $x = 0$, the axial velocity for $x > 0$ becomes

$$u = \overline{u} - \epsilon u_o + \epsilon u_o e^{+\pi \frac{x}{b}} \int_0^a f(\xi)\, e^{-\pi \frac{x}{b}} d\xi . \tag{20}$$

for $0 < x < a$,

$$u = \overline{u} + \epsilon u_o \left\{ \int_0^x f(\xi) \left[1 - e^{-\frac{\pi}{b}(x-\xi)} \right] d\xi - \int_x^a f(\xi) \left[1 - e^{+\frac{\pi}{b}(x-\xi)} \right] d\xi \right\} . \tag{21}$$

For $x > a$,

$$u = \bar{u} + \varepsilon u_o - \varepsilon u_o e^{-\pi \frac{x}{b}} \int_0^a f(\xi) e^{+\pi \frac{x}{b}} d\xi . \qquad (22)$$

The equations for a rotor are similar with only the algebraic sign of u_o changed throughout.

Equations (20) - (22) give the flow due to one blade row alone. For a repeating flow pattern, the velocities are the same as if there were an infinite number of blade rows. Thus, for the complete flow pattern, we must superimpose the flows due to many stators and many rotors. The following definitions will be used:

a_s = width of a stator row

a_r = width of a rotor row

c_s = gap between stator and rotor

c_r = gap between rotor and stator

$f_s(\xi)d\xi$ = fraction of disturbance due to stator

$f_r(\xi)d\xi$ = fraction of disturbance due to rotor

$\ell = a_s + c_s + a_r + c_r$

The leading edge of the stators are then set at

$$x = m\ell \qquad \text{where} \qquad m = 0, \pm 1, \pm 2, \ldots$$

and the leading edges of the rotors are at

$$x = a_s + c_s + m\ell .$$

The axial velocity in a stator row due to all blades becomes

$$u = \overline{u}(y) + \epsilon u_o(y) \left\{ \int_0^x f_s(\xi) \left[1 - e^{-\frac{\pi}{b}(x-\xi)}\right] d\xi - \int_x^{a_s} f_s(\xi) \left[1 - e^{+\frac{\pi}{b}(x-\xi)}\right] d\xi \right\}$$

$$- \epsilon \sum_{m=0}^{\infty} u_o(y) \int_0^{a_r} f_r(\xi)\, e^{-\pi \frac{\xi}{b}} d\xi \; e^{\frac{\pi}{b}[x-a_s-c_s-m\ell]}$$

$$+ \epsilon \sum_{m=1}^{\infty} u_o(y) \int_0^{a_r} f_r(\xi)\, e^{+\pi \frac{\xi}{b}} d\xi \; e^{-\frac{\pi}{b}[x-m\ell]}$$

$$+ \epsilon \sum_{m=1}^{\infty} u_o(y) \int_0^{a_s} f_s(\xi)\, e^{-\pi \frac{\xi}{b}} d\xi \; e^{+\frac{\pi}{b}[x-m\ell]}$$

$$- \epsilon \mathop{}_{m=1}^{\infty} u_o(y) \int_0^{a_s} f_s(\xi)\, e^{+\pi \frac{\xi}{b}} d\xi \; e^{-\frac{\pi}{b}[x+m\ell]} \quad . \qquad (23)$$

Carrying out the summations, equation (23) becomes

$$u = \overline{u}(y) + \epsilon u_o(y) \left\{ \int_0^x f(\xi) \left[1 - e^{-\frac{\pi}{b}(x-\xi)}\right] d\xi - \int_x^{a_s} f(\xi) \left[1 - e^{+\frac{\pi}{b}(x-\xi)}\right] d\xi \right\}$$

$$- \frac{\epsilon u_o(y)}{1 - e^{-\frac{\pi}{b}\ell}} \left\{ \int_0^{a_r} f_r(\xi)\, e^{-\pi \frac{\xi}{b}} d\xi \; e^{\pi \frac{x}{b}} \; e^{-\frac{\pi}{b}(a_s+c_s)} \right.$$

$$- \int_0^{a_r} f_r(\xi)\, e^{+\pi \frac{\xi}{b}} d\xi \; e^{-\pi \frac{x}{b}} \; e^{-\frac{\pi}{b}(a_r+c_r)} - \int_0^{a_s} f_s(\xi)\, e^{-\pi \frac{\xi}{b}} d\xi \; e^{\pi \frac{x}{b}} \; e^{-\frac{\pi}{b}\ell}$$

$$\left. + \int_0^{a_s} f_s(\xi)\, e^{+\pi \frac{\xi}{b}} d\xi \; e^{-\pi \frac{x}{b}} \; e^{-\frac{\pi}{b}\ell} \right\} \quad . \qquad (24)$$

For the axial velocity in a rotor row, change the sign of u_o and interchange the s and r subscripts in all terms of equation (24).

The corresponding calculation of the whirl velocity in a stator results in

$$\begin{aligned}
w = \bar{w}(y) &+ \epsilon \int_0^x f_s(\xi)\left[w_o(y) - \frac{1}{\bar{u}}\frac{d\bar{w}}{dy}\int_0^y u_o(\eta)d\eta \; e^{-\frac{\pi}{b}(x-\xi)}\right]d\xi \\
&- \epsilon \int_x^{a_s} f_s(\xi)\left[w_o(y) - \frac{1}{\bar{u}}\frac{d\bar{w}}{dy}\int_0^y u_o(\eta)d\eta \; e^{+\frac{\pi}{b}(x-\xi)}\right]d\xi \\
&- \epsilon \frac{1}{\bar{u}}\frac{d\bar{w}}{dy}\int_0^y u_o(\eta)d\eta \; \frac{1}{1 - e^{-\frac{\pi \ell}{b}}} \left\{ \int_0^{a_r} f_r(\xi)\, e^{-\pi\frac{\xi}{b}} d\xi \; e^{\pi\frac{x}{b}} \; e^{-\frac{\pi}{b}(a_s+c_s)} \right. \\
&- \int_0^{a_r} f_r(\xi)\, e^{+\pi\frac{\xi}{b}} d\xi \; e^{-\pi\frac{x}{b}} \; e^{-\frac{\pi}{b}(a_r+c_r)} - \int_0^{a_s} f_s(\xi)\, e^{-\pi\frac{\xi}{b}} d\xi \; e^{\pi\frac{x}{b}} \; e^{-\pi\frac{\ell}{b}} \\
&\left. + \int_0^{a_s} f_s(\xi)\, e^{+\pi\frac{\xi}{b}} d\xi \; e^{-\pi\frac{x}{b}} \; e^{-\pi\frac{\ell}{b}} \right\} . \qquad (25)
\end{aligned}$$

The whirl velocity in a rotor is determined by changing the sign of u_o and w_o and interchanging the s and r subscripts in equation (25).

An example will be shown later for which the following assumptions are made:

$a_s = a_r = a$,

$c_s = c_r = c$,

$f_s(\xi) = f_r(\xi) = 1/a$,

$\ell = 2(a + c)$.

D. Flow Patterns for Blading of High Aspect Ratio

If then the exponentials are expanded in polynomials of a/b , c/b , or x/b , as the case may be, and terms through second order are

retained, the velocities reduce to

$$\begin{aligned} u &= \bar{u} + \epsilon u_o \pi \left(\frac{x}{b} - \frac{a}{2b} \right) \\ w &= \bar{w} + \epsilon w_o \left(2\frac{x}{a} - 1 \right) - \epsilon \Gamma \left(2\frac{x}{a} - 1 - \frac{\pi x}{b} + \frac{\pi a}{b} \right) \end{aligned} \tag{26}$$

for a stator, and

$$\begin{aligned} u &= \bar{u} - \epsilon u_o \pi \left(\frac{x}{b} - \frac{a}{2b} \right) \\ w &= \bar{w} - \epsilon w_o \left(2\frac{x}{a} - 1 \right) + \epsilon \Gamma \left(2\frac{x}{a} - 1 - \frac{\pi x}{b} + \frac{\pi a}{2b} \right) \end{aligned} \tag{27}$$

for a rotor. In both cases

$$\Gamma = \frac{1}{\bar{u}} \frac{d\bar{w}}{dy} \int_0^y u_o(\eta)\, d\eta \quad . \tag{28}$$

The entering and leaving flow angles for both stator and rotor blades can now be calculated. The defining equations for these angles are, in the case of a stator,

$$\tan \gamma_1 = \frac{u(x = 0)}{w(x = 0)}$$

and

$$\tan \gamma_2 = \frac{u\,(x = a)}{w\,(x = a)} \tag{29}$$

where γ_1 is the stator entering angles and γ_2 is the stator leaving angle. For the rotor,

$$\tan \beta_1 = \frac{u(x = 0)}{\text{blade speed} - w(x=0)}$$

and

$$\tan \beta_2 = \frac{u(x = a)}{\text{blade speed} - w(x=a)} \quad .$$

In summary, given the blade loading, blade aspect ratio, the axial velocity through the compressor, the whirl velocity at one radius of a blade row, the desired pressure rise across a stage, and the desired degree of reaction, one can compute the shape of the blades subject

to the restriction that they be of high aspect ratio and very closely spaced.

III. THEORY FOR FINITE HUB RADIUS

The analysis for the limiting case of hub ratio equal to one is extended to the axisymmetric case of finite hub radius with only slight modifications. The y coordinate goes over into the radius r. The velocity in the r direction remains v. The major change here is that the radial pressure gradients must be accounted for properly.

The equations of motion in the axisymmetric case are

$$
\begin{aligned}
&\frac{\partial u}{\partial r} + \frac{1}{r}\frac{\partial}{\partial r}(rv) = 0 \\
&u\frac{\partial u}{\partial x} + v\frac{\partial u}{\partial r} = -\frac{1}{\rho}\frac{\partial p}{\partial x} \\
&u\frac{\partial v}{\partial x} + v\frac{\partial v}{\partial r} - \frac{w^2}{r} = -\frac{1}{\rho}\frac{\partial p}{\partial r} \\
&u\frac{\partial w}{\partial x} + v\frac{\partial w}{\partial r} + \frac{vw}{r} = 0
\end{aligned}
\qquad (31)
$$

As before, we assume a perturbation approach of the form

$$
\begin{aligned}
u &= \overline{u}(r) \mp \epsilon u_o(r) + \epsilon u_1(x, r) \\
v &= \epsilon v_1(x, r) \\
w &= \overline{w}(r) \mp \epsilon w_o(r) + \epsilon w_1(x, r) \\
p &= \overline{p}(r) \mp \epsilon p_o(r) + \epsilon p_1(x, r)
\end{aligned}
\qquad (32)
$$

Notice that $\overline{p}$ and p_o are now functions of the radial variable, r.

The resulting linear equations are

$$
\begin{aligned}
&\frac{\partial u_1}{\partial x} + \frac{1}{r}\frac{\partial}{\partial r}(rv_1) = 0 \\
&\overline{u}\frac{\partial u_1}{\partial x} + v_1\frac{\partial \overline{u}}{\partial r} = -\frac{1}{\rho}\frac{\partial p_1}{\partial x} \\
&\overline{u}\frac{\partial v_1}{\partial x} - 2\frac{\overline{w}\,w_1}{r} = -\frac{1}{\rho}\frac{\partial p_1}{\partial r} \\
&\overline{u}\frac{\partial w_1}{\partial x} + v_1\frac{\partial \overline{w}}{\partial r} + \frac{v_1\overline{w}}{r} = 0
\end{aligned}
\qquad (33)
$$

and also the radial pressure equilibrium equations

$$\frac{1}{\rho}\frac{\partial \bar{p}}{\partial r} = \frac{\bar{w}^2}{r} \tag{34}$$

and

$$\frac{1}{\rho}\frac{\partial p_o}{\partial r} = \frac{2\bar{w}\, w_o}{r}$$

which must be satisfied at $x = \pm \infty$.

Eliminating the other dependent variables, the equation for v_1 becomes

$$\frac{\partial^2 v_1}{\partial x^2} + \frac{\partial^2 v_1}{r} + \frac{1}{r}\frac{\partial v_1}{\partial r} - [\frac{1}{r^2} + F(r)]v_1 = 0 , \tag{35}$$

where

$$F(r) = \frac{r}{\bar{u}}\frac{d}{dr}\left(\frac{1}{r}\frac{d\bar{u}}{dr}\right) - \frac{2}{r^2}\frac{\bar{w}}{\bar{u}^2}\frac{d}{dr}(r\bar{w}) .$$

An appropriate solution is of the form

$$v_1 = e^{\pm\lambda \frac{x}{b}} R(r) .$$

Substituting into equation (35) yields

$$R'' + \frac{1}{r} R' + [(\frac{\lambda}{b})^2 - \frac{1}{r^2} - F(r)]R = 0 \tag{36}$$

where the prime indicates differentiation with respect to r . If $F(r)$ is chosen identically equal to zero, then (36) reduces to Bessel's equation. If we then take only the first term of the solution for v_1 , the boundary condition that $v = 0$ at the hub and the tip gives, for the first eigenvalue

$$\lambda_1 = 3.18$$

for a hub ratio of 0.6 . If $F(r)$ is small compared to $(\lambda_1/b)^2$, then the first eigenvalue does not change substantially. We will now choose $F(r)$ identically equal to zero and later compute its actual value to

compare with $(\lambda_1/b)^2$.

Proceeding as in the case with infinite hub radius, the perturbation quantities become

$$
\begin{aligned}
u_1 &= \pm u_o \, e^{\pm\lambda \frac{x}{b}} \\
v_1 &= -\frac{1}{r}\frac{\lambda}{b}\, e^{\pm\lambda \frac{x}{b}} \int_{r_i}^{r} \eta\, u_o(\eta)\, d\eta \\
w_1 &= \pm\frac{1}{\bar{u}}\left(\frac{d\bar{w}}{dr} + \frac{\bar{w}}{r}\right)\frac{1}{r}\, e^{\pm\lambda \frac{x}{b}} \int_{r_i}^{r} \eta\, u_o(\eta)\, d\eta \\
\frac{p_1}{\rho} &= \mp e^{\pm\lambda \frac{x}{b}}\left[\bar{u} u_o - \frac{1}{r}\frac{d\bar{u}}{dr}\int_{r_i}^{r} \eta\, u_o(\eta)\, d\eta\right]
\end{aligned}
\qquad (37)
$$

where r_i is the hub radius.

The condition that the total pressure rise across a disk be a constant yields

$$
\frac{\Delta p_T}{\rho} = 2\epsilon\,\frac{p_o}{\rho} + 2\epsilon(\bar{u} u_o + \bar{w} w_o) - 2\epsilon\left[\frac{1}{r}\frac{d\bar{u}}{dr} + \frac{\bar{w}}{\bar{u} r}\left(\frac{d\bar{w}}{dr} + \frac{\bar{w}}{r}\right)\right]\int_{r_i}^{r} \eta\, u_o(\eta)\, d\eta . \quad (38)
$$

Again choosing the special condition of constant total pressure in the radial direction implies to first order in ϵ that

$$
\bar{p} + \tfrac{1}{2}\rho\,(\bar{w}^2 + u^2) = K_1
$$

and (39)

$$
p_o + \rho\,(\bar{w} w_o + \bar{u} u_o) = K_2 .
$$

Then, as in the simpler case, equation (38) applied across a stator requires $K_2 = 0$. Combining equations (34) and (39) results in the two conditions

$$\frac{1}{r^2}\frac{d}{dr}(r\bar{w})^2 = -\frac{d\bar{u}^2}{dr}$$

and (40)

$$\frac{d}{dr}(r^2\bar{w}w_o) = -r^2\frac{d}{dr}(\bar{u}u_o) .$$

The remainder of the analysis, consisting of the summation of the disturbances due to the disks in order to produce a finite blade and the summation over all blade rows to derive the complete flow pattern for the compressor, proceeds exactly as in the limiting case, and only results will be given here. With the definition

$$\Gamma = \frac{1}{r\bar{u}}\left(\frac{d\bar{w}}{dr} + \frac{\bar{w}}{r}\right)\int_{r_i}^{r} \eta\, u_o(\eta)\, d\eta ,$$

the velocity components for the stators are

$$u = \bar{u} + \epsilon u_o \lambda\left(\frac{x}{b} - \frac{a}{2b}\right)$$

and (41)

$$w = \bar{w} + \epsilon w_o\left(2\frac{x}{a} - 1\right) - \epsilon\Gamma\left(2\frac{x}{a} - 1 - \frac{\lambda x}{b} + \frac{\lambda a}{2b}\right),$$

and for the rotors

$$u = \bar{u} - \epsilon u_o \lambda\left(\frac{x}{b} - \frac{a}{2b}\right)$$

and (42)

$$w = \bar{w} - \epsilon w_o\left(2\frac{x}{a} - 1\right) + \epsilon\Gamma\left(2\frac{x}{a} - 1 - \frac{\lambda x}{b} + \frac{\lambda a}{2b}\right).$$

The blade angles are determined exactly as before with the use of equations (28) and (29).

IV. AN APPLICATION OF THE THEORY

Before proceeding with an example that will allow us to verify this theory against an existing compressor, we will indicate the steps in order.

1. Choose the blade loading function $f(\xi)$ for both the rotor and the stator.

2. Choose the blade dimensions.

3. Solve equation (36) for the eigenfunctions and determine the eigenvalues by application of the boundary conditions on the radial velocity v. For many applications, $F(r)$ can be taken equal to zero and all constants in the series solution for v taken equal to zero except the first ones. For such applications, the magnitude of λ_1 will be approximately π.

4. Continue the summation procedures that result in relations similar to equations (41) and (42).

5. Pick $\overline{u}$ and u_o. Notice u_o must satisfy the condition that

$$\int_{r_i}^{r_o} r\, u_o\, dr = 0$$

where r_i and r_o are the inner and outer boundaries of the cylindrical annulus.

6. Determine $\overline{w}$ from the first of equations (40). There will remain an undetermined constant to choose.

7. Choose the pressure rise across a stage and the degree of reaction desired. The pressure rise across a stator $2p_o$ can then be determined.

8. Determine w_o from the second of equations (40). The undetermined constant is then evaluated by use of the second of equations (39).

9. Evaluate the function ϕ .

10. Calculate the axial and whirl velocities for both the stator and rotor by using the equations derived in step 4.

11. Compute the blade angles by use of equations (28) and (29).

It was decided to use this theory to compare with the blade design given in Ref. 1 for solid body blading. The steps will be taken as listed above and the results presented here and in Table 1 on page 58.

1. The loading function was taken to be constant for ease in computation. A triangular distribution would be more nearly correct.

2. The ratio a/b was taken to be $1/3$.

3. $F(r)$ was taken equal to zero and λ_1 found to be approximately 3.18 . The function $F(r)$ was subsequently checked and found negligible compared to $(\lambda/b)^2$.

4. Equations (41) and (42) were then correct as stated in the theory.

5. $\overline{u}$ and u_o were then chosen to approximate as closely as possible the axial flow used in the design of the solid body blading in Ref. 1. The relations were

$$\overline{u}/u_T = -.560\,\xi + .916$$

and

$$u_o/u_T = .185\,\xi - .151$$

where ξ is a non-dimensional radius based on the tip radius and u_T is the rotor tip speed.

6. Equation (40) was used to determine $\overline{w}$ in the form

$$\left(\frac{\bar{w}}{u_T}\right)^2 = .342\,\xi - .157\,\xi^2 - \frac{c_1}{\xi^2} .$$

The constant c_1 was determined by choosing $\bar{w} = .385$ at $\xi = 0.8$.

7. The ideal pressure coefficient for the compressor was 0.40. Then by definition

$$\frac{p_s}{\rho} + \frac{p_r}{\rho} = \frac{0.40}{2} u_T^2$$

where u_T is the blade tip speed that has been used throughout this analysis in order to non-dimensionalize the velocity components. Fifty per cent reaction in this compressor occurred at $\xi = 0.8$. Since $2p_o = p_s$, we obtained the following relation

$$p_o/\rho = 0.05\,u_T^2 .$$

8. The equation for w_o then became

$$\frac{w_o}{u_T} = \frac{1}{\bar{w}/u_T}\left(.052\,\xi^2 - .085\,\xi - \frac{.009}{\xi^2}\right) .$$

9. The function ϕ was evaluated numerically and is listed in Table 1.

10. and 11. The values of u and w are listed in Table 1 for different values of ξ . Similarly, the entering and leaving angles γ_1 , γ_2 , β_1 , and β_2 are tabulated. The values of these angles used in the original design are also tabulated.

V. CONCLUDING REMARKS

For most compressor designs occurring in practice, the aspect ratio of the blades is neither very low nor very high. It falls somewhere in between. The theory of Part I of this thesis is applicable for blading of low aspect ratio, where it is assumed that equilibrium flow patterns exist at the leading and trailing edges of the blade rows. A blade row is not affected by neighboring blade rows except through the incident velocity distributions. The theory of Part II for blades of high aspect ratio contains the influence of disturbances of potential type that can be felt upstream as well as downstream.

The close agreement between the results of the two theories for an aspect ratio of three indicates that there the flow between blades is very near its equilibrium state at the leading and trailing edges.

REFERENCES FOR PART II

1. Marble, F. E., "The Flow of a Perfect Fluid Through an Axial Turbomachine with Prescribed Blade Loading," Journal of Aero. Sci., Vol. 15, pp. 473-485 (August, 1948).

2. Bowen, J. T., Sabersky, R. H., and Rannie, W. D., "Theoretical and Experimental Investigations of Axial-Flow Compressors," Report on Research Conducted under Contract with the Office of Naval Research, California Institute of Technology, Pasadena (January, 1949).

TABLE I

CALCULATION OF FLOW ANGLES

	ξ	0.6	0.7	0.8	0.9	1.0
Stator Blades	$\overline{u}$	0.580	0.524	0.468	0.412	0.356
	u_o	-0.040	-0.022	-0.003	+0.016	+0.034
	$\overline{w}$	0.322	0.360	0.385	0.402	0.412
	w_o	-0.177	-0.143	-0.127	-0.114	-0.102
	Γ	0	-0.004	-0.005	-0.003	0
	$u\ (x=0)$	0.601	0.536	0.470	0.404	0.338
	$w\ (x=0)$	0.499	0.501	0.510	0.515	0.514
	γ_1	50.3^o	46.9^o	42.7^o	38.1^o	33.3^o
	$u\ (x=a)$	0.559	0.512	0.466	0.420	0.374
	$w\ (x=a)$	0.145	0.219	0.260	0.289	0.310
	γ_2	75.4^o	66.8^o	60.8^o	55.5^o	50.4^o

TABLE I (cont'd.)

CALCULATION OF FLOW ANGLES

Rotor Blades	$u\,(x=0)$	0.559	0.512	0.466	0.420	0.374
	$\omega\xi - w\,(x=0)$	0.455	0.481	0.540	0.611	0.690
	β_1	50.8°	46.8°	40.8°	34.5°	28.5°
	$u\,(x=a)$	0.601	0.536	0.470	0.404	0.338
	$\omega\xi - w\,(x=a)$	0.101	0.199	0.290	0.385	0.486
	β_2	80.5°	69.6°	58.3°	46.4°	34.8°
Low Aspect Ratio Design	γ_1	48.4°	46.3°	42.7°	37.4°	29.3°
	γ_2	69.5°	65.3°	60.6°	55.2°	48.7°
	β_1	52.2°	46.3°	40.5°	34.7°	28.7°
	β_2	83.1°	70.8°	58.3°	45.6°	31.8°

thesM384
Part I. Analysis of a multi-stage axial
3 2768 002 12542 9
DUDLEY KNOX LIBRARY